

Article

Not peer-reviewed version

Vacuum Expansion and Collapse Inside an Infinite Shell

[Christopher Laforet](#) *

Posted Date: 24 July 2023

doi: 10.20944/preprints202201.0301.v17

Keywords: Cosmology; Black holes; Dark Energy; Schwarzschild metric



Preprints.org is a free multidiscipline platform providing preprint service that is dedicated to making early versions of research outputs permanently available and citable. Preprints posted at Preprints.org appear in Web of Science, Crossref, Google Scholar, Scilit, Europe PMC.

Copyright: This is an open access article distributed under the Creative Commons Attribution License which permits unrestricted use, distribution, and reproduction in any medium, provided the original work is properly cited.

Article

Vacuum Expansion and Collapse Inside an Infinite Shell

Christopher A. Laforet

address

Abstract: The FRW model of cosmology assumes a Universe with uniform pressure and density everywhere in space at a given time. But at the largest scales, the Universe has a web-like structure surrounding large voids, violating these assumptions. Furthermore, a given region of spacetime is describable only by a single metric and therefore it cannot be that the Universe is modelled as an FRW perfect fluid since this would be the incorrect description of both the web and the voids. The cosmic web must be described by metrics with non-zero energy-momentum tensors with non-uniform pressure and density describing the matter within it. Therefore, the model of cosmology describing the expansion of the Universe must be a vacuum solution describing the empty spaces in the Universe surrounded by an infinite, massive shell (the surrounding Universe). The internal Schwarzschild metric is the model for these vacua. A detailed analysis of falling frames in the external metric in Kruskal-Szekeres coordinates shows that the source of the Schwarzschild metric is at the event horizon, a location/time of infinite density, not at the singularity, as it is currently assumed. The spatial homogeneity of the internal metric is demonstrated by visualizing the geometry in Kruskal-Szekeres coordinates (visualized in 1+2 dimensions) as well as examining the Killing vectors for the internal spacetime. Using the coordinate age of the Universe and transition redshift, this predicts the accelerated expansion, the Hubble diagram fits currently available cosmological data, and it gives a Hubble constant H_0 of 71.6 km/s/Mpc . The angular term of the metric describes the relativistic kinematic precession effect known as Thomas Precession which can be interpreted as spin about the time dimension.

Keywords: cosmology; general relativity; schwarzschild; black holes; dark energy; dark matter

1. Motivation and Roadmap

The current model of cosmology is based on the FRW metric, which comes from the assumption that the Universe is accurately modelled as perfect fluid. This means that we are modelling the Universe as having uniform density and pressure at all points in space. While this may be a good approximation for the early pre-recombination Universe, the perfect fluid assumption is clearly no longer a valid one in the later Universe. We observe that the Universe is not a uniform distribution of galaxies, but rather a web-like structure of matter surrounding large voids. Thus, the pressure and density is surely not uniform at all locations in space, making the perfect fluid assumption less and less accurate as the Universe expands and cools.

Furthermore, it is notable that a given region of spacetime can only be described by one metric. This means that the region containing a star, for example, is not described by the FRW metric, it is described by a spherically-symmetric metric with a radially-dependant mass density and pressure where the metric must match the external Schwarzschild metric at the star's outer radius. Therefore, the cosmic filaments cannot be described by the FRW metric because they are not perfect fluids (with regions of uniformly dense gas being the exception) and the spacetime in those regions will be described by metrics whose mass distribution matches the configurations of the filaments. What this implies is that a cosmological metric (one that accurately describes the expansion of the Universe) must be a vacuum solution describing the empty spaces surrounded by the matter in the Universe. This empty space differs from Minkowski space in that the empty spaces in the Universe are surrounded by

the infinite mass of the Universe and therefore should be modelled as a spherically-symmetric vacuum surrounded by a shell of infinite mass.

It will be argued in this paper that the metric properly describing the vacuum of the Universe, including its accelerated expansion, is the *internal* Schwarzschild metric. Sections 3 and 4 demonstrate how the source of both the external and internal metrics are not at $r = 0$, but rather at the event horizon which represents an infinitely dense shell as viewed from the outside in the case of the external metric, and an infinitely dense shell as viewed from the inside in the case of the internal metric. The justification for the mass not being concentrated at $r = 0$ is also supported by the fact that if this were true, it would violate the vacuum assumption of the metric. Justification for the internal metric representing a vacuum surrounded by a shell at infinity comes from looking at the geometry in Kruskal coordinates and noting that the horizon is located at spatial infinity for the internal metric. This means that in the internal metric, the shell has an infinite Schwarzschild radius and therefore infinite mass. In both metrics, as will be shown, these shells look like infinitely dense points in the frame of an observer approaching the shell in space for the case of the external metric and in time for the case of the internal metric. The temporal nature of the spatial expansion and contraction of the internal metric matches what we observe in regards to the structure of the Universe.

In Section 3, we define the Lorentz boost and Rapidity for falling frames of the external metric in Kruskal-Szekeres coordinates by finding the relative velocity between the rest frame and falling frame in these coordinates. The analysis of the Kruskal-Szekeres coordinate differentials leads to an expression that gives the full Kruskal-Szekeres derivative as the relativistic velocity addition of the velocity of the rest frame and the relative velocity between the rest frame and falling frame in Kruskal-Szekeres coordinates. The velocity of the rest frame is a function of only the Schwarzschild time t and since the Schwarzschild metric is independent of t this velocity is merely a coordinate artifact and does not correspond to a physical velocity. By solving for the relative velocity between the rest frame and falling frame in Kruskal-Szekeres coordinates, we are able to define the Lorentz boost in Kruskal-Szekeres coordinates of the falling frame relative to the rest frame and find that at the horizon, the entire spacetime is length contracted in the falling frame as the horizon is approached, such that there is no spacetime inside the horizon in that frame. This bolsters the conclusion that the internal metric is not describing the inside of a black hole, but rather infinite space surrounded by an infinitely dense shell located at a past time in the frame of a present observer. The rest of the paper provides detailed analysis of the internal metric spacetime and its cosmological consequences.

In Section 4, we also demonstrate that surfaces of constant time in the internal metric can be visualized as a collection of 2-sheeted hyperboloids analogous to how the external metric at a given radius can be visualized as a collection of one sheet hyperboloids. The 2-sheeted hyperbolic nature of the metric changes the interpretation of the angular term relative to the external metric, and it is shown that the metric describes a Universe that is isotropic, homogeneous in space and inhomogeneous in time, as our Universe has been observed to be. The homogeneity of space of the internal metric is demonstrated by analyzing the Killing vectors in the context of the internal metric. It is also demonstrated that the angular term of the internal metric comes from the kinematic relativistic effect known as Thomas Precession. This precession acts as an intrinsic 'spin' around the time dimension. In Section 5, it is shown how this term gives rise to Coriolis accelerations that affect curvilinear motion of massive objects as well as gravitational lensing angles.

In Section 8 we solve for the unknowns for the internal Schwarzschild metric, namely our current cosmological position in the metric and the counterpart of the Schwarzschild radius, using existing cosmological data. The model is then used to calculate relevant cosmological parameters and it is found that the model fits the cosmological data very well.

In Section 12, we place the external metric in the background cosmology of the internal metric and show that a Black Hole event horizon can never form during the expansion phase. We see that gravity becomes repulsive during the collapse phase and would-be Black Holes become White Holes.

This is a consequence of the Universe moving in the opposite direction of time during collapse relative to expansion.

We will begin the argument by examining the geometry of the full Schwarzschild metric in detail.

2. The Schwarzschild Metric in Schwarzschild and Kruskal-Szekeres Coordinates

The event horizon of the Schwarzschild metric is described as a coordinate singularity in Schwarzschild coordinates. This singularity is overcome using the Kruskal-Szekeres coordinates for the spacetime since the metric is regular at the horizon. However, the meaning of the the Kruskal-Szekeres coordinates in terms of spacelike and timelike basis vectors is not clear. For much of the spacetime, the Kruskal-Szekeres coordinates are mixtures of space and time such that the meaning of the slope of a worldline in these coordinates is not always clear.

In this paper, the Kruskal-Szekeres coordinates and the derivatives of worldlines in these coordinates is clarified. We find that we can define a Lorentz boost and rapidity in Kruskal-Szekeres coordinates for falling frames, and with those, it is shown that the worldlines of all frames approaching the event horizon become light-like there, even if the slope of the worldline in Kruskal-Szekeres coordinates is not ± 1 there. This is possible because the derivative of the worldline in Kruskal-Szekeres coordinates at the horizon is not a true velocity due to the fact that the coordinates are mixtures of space and time. But we can mathematically extract a derivative for the worldline in Kruskal-Szekeres coordinates which is a true velocity relative to the rest frame for any point on the worldline by removing the part of the derivative related to the rest frame at the same point, and we find that this velocity goes to 1 at the horizon for all worldlines.

3. The Falling Frame of the External Metric in Kruskal-Szekeres Coordinates

The Schwarzschild metric is the simplest non-trivial solution to Einstein's field equations. It is the metric that describes every spherically symmetric vacuum spacetime. The the external form of the metric can be expressed as:

$$d\tau^2 = \left(1 - \frac{r_s}{r}\right) dt^2 - \frac{1}{1 - \frac{r_s}{r}} dr^2 - r^2 d\Omega^2 \quad (1)$$

Equation 1 is the external metric with t being the timelike coordinate and r being the spacelike coordinate. The Schwarzschild radius of the metric is given by $r_s = 2GM$ in units with $c = 1$. The external metric is the metric for an eternally spherically-symmetric vacuum centered in space.

We can see in Equation 1 that as $r \rightarrow r_s$, the magnitude of the basis vector ∂_t goes to zero while the magnitude of ∂_r goes to infinity. This location is called the 'Event Horizon' of the metric. The behaviour of the basis vectors at this location seem to imply that there is a coordinate singularity at this location since the spacetime curvature is not infinite there.

In order to overcome the behaviour of the basis vectors at this location, different coordinate systems have been developed which do not have degenerate behaviour at the Event Horizon. The most important of these coordinate systems are the Kruskal-Szekeres coordinates, which are the maximally extended coordinates for the Schwarzschild metric. The coordinate definitions and metric in Kruskal-Szekeres coordinates are given below (derivation of the coordinate definitions and metric can be found in reference [1] where $v = T$ and $u = X$).

$$\begin{aligned} T &= \sqrt{\left(\frac{r}{r_s} - 1\right)} e^{\frac{r}{r_s}} \sinh\left(\frac{t}{2r_s}\right) \\ X &= \sqrt{\left(\frac{r}{r_s} - 1\right)} e^{\frac{r}{r_s}} \cosh\left(\frac{t}{2r_s}\right) \end{aligned} \quad (2)$$

With the full metric in Kruskal-Szekeres coordinates given by:

$$d\tau^2 = \frac{4r_s^3}{r} e^{-\frac{r}{r_s}} (dT^2 - dX^2) - r^2 d\Omega^2 \quad (3)$$

Finally, we plot the metric on the Kruskal-Szekeres coordinate chart [2] in Figure 1:

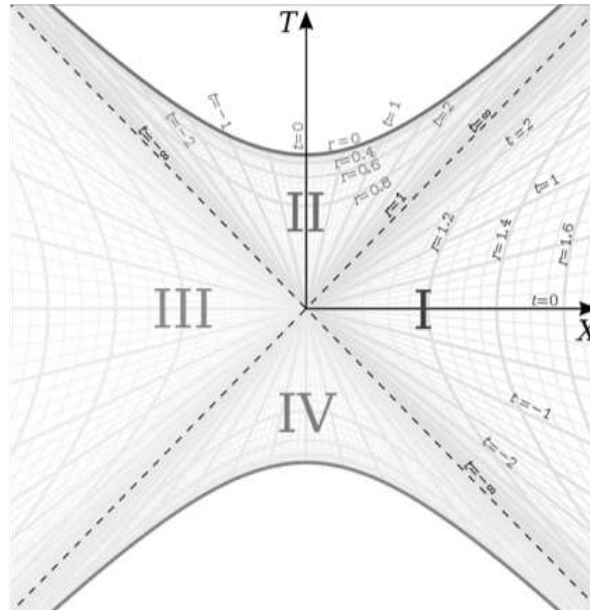


Figure 1. Kruskal-Szekeres Coordinate Chart

In this section, we will be focusing on region I in this chart, which is the spherically symmetric spacetime around a spherically symmetric source in space.

We can see in Figure 1 that for a rest frame ($r = \text{const}$), that $\frac{dX}{dT}$ depends on the value of t we evaluate the derivative at since the derivative for the rest frame is the tangent to the hyperbola at t . Since the metric is time-symmetric, we know that the actual physics does not depend on the value of t and therefore, we need a deeper understanding of the meaning of the changing $\frac{dX}{dT}$ in the rest frame and how it relates to the falling frame at the same point.

Let us first take the differentials of T and X in Equation 2:

$$\begin{aligned} dX &= \frac{\partial X}{\partial r} dr + \frac{\partial X}{\partial t} dt \\ dT &= \frac{\partial T}{\partial r} dr + \frac{\partial T}{\partial t} dt \end{aligned} \quad (4)$$

Calculating the partial derivatives, rearranging and defining $R \equiv \frac{re^{\frac{r}{r_s}}}{2r_s \sqrt{(\frac{r}{r_s}-1)e^{\frac{r}{r_s}}}}$ we get:

$$\begin{aligned} \frac{dX}{dt} &= R \left[\frac{dr}{dt} \cosh\left(\frac{t}{2r_s}\right) + \left(1 - \frac{r_s}{r}\right) \sinh\left(\frac{t}{2r_s}\right) \right] \\ \frac{dT}{dt} &= R \left[\frac{dr}{dt} \sinh\left(\frac{t}{2r_s}\right) + \left(1 - \frac{r_s}{r}\right) \cosh\left(\frac{t}{2r_s}\right) \right] \end{aligned} \quad (5)$$

Next, we need to calculate $\frac{dX}{dT}$ from equations 5 by factoring out $(1 - \frac{r_s}{r}) \cosh\left(\frac{t}{2r_s}\right)$ from each equation and dividing:

$$\frac{dX}{dT} = \frac{dX}{dt} \frac{dt}{dT} = \frac{\frac{dr}{dt} (1 - \frac{r_s}{r})^{-1} + \tanh\left(\frac{t}{2r_s}\right)}{\frac{dr}{dt} (1 - \frac{r_s}{r})^{-1} \tanh\left(\frac{t}{2r_s}\right) + 1} \quad (6)$$

Next, we make the following definitions:

$$\left(\frac{dX}{dT}\right)_0 \equiv \tanh\left(\frac{t}{2r_s}\right) \quad (7)$$

This is the derivative of the rest frame at t since plugging $\frac{dr}{dt} = 0$ into Equation 6, we get $\frac{dX}{dT} = \tanh\left(\frac{t}{2r_s}\right)$. Since we know the Schwarzschild metric is independent of t , this derivative must represent the flow of the spacetime itself in these coordinates (it is a non-physical artifact of the Kruskal-Szekeres coordinates) at fixed r and is not related to any actual change in motion through space and time.

And we define the relative velocity of the frame in motion relative to the rest frame as:

$$\left(\frac{dX}{dT}\right)_{rel} \equiv \frac{dr}{dt} \left(1 - \frac{r_s}{r}\right)^{-1} \quad (8)$$

This is the relative velocity in Kruskal-Szekeres coordinates between the frame in motion and the rest frame at r . This derivative is 0 for the rest frame since $\frac{dr}{dt} = 0$ in that frame. Note that this derivative seems to be problematic at $r = r_s$, except that reference [3] tells us that $\frac{dr}{dt}$ for an observer falling from rest at $r = r_0$ is given by:

$$\frac{dr}{dt} = -\left(1 - \frac{r_s}{r}\right) \sqrt{\frac{\frac{r_s}{r} - \frac{r_s}{r_0}}{1 - \frac{r_s}{r_0}}} \quad (9)$$

And if we combine equations 8 and 9 we get:

$$\left(\frac{dX}{dT}\right)_{rel} = -\sqrt{\frac{\frac{r_s}{r} - \frac{r_s}{r_0}}{1 - \frac{r_s}{r_0}}} \quad (10)$$

Which is well behaved and equal to -1 when $r = r_s$. Plugging these definitions into Equation 6, we get:

$$\frac{dX}{dT} = \frac{\left(\frac{dX}{dT}\right)_{rel} + \left(\frac{dX}{dT}\right)_0}{\left(\frac{dX}{dT}\right)_{rel} \left(\frac{dX}{dT}\right)_0 + 1} \quad (11)$$

We recognize that Equation 11 is the relativistic velocity addition formula giving us the total velocity as the relativistic sum of the rest frame velocity and the relative velocity between the moving frame and the rest frame. We can solve for $\left(\frac{dX}{dT}\right)_{rel}$ to get an expression for the relative velocity between a frame in motion and the rest frame in Kruskal-Szekeres coordinates:

$$\left(\frac{dX}{dT}\right)_{rel} = -\frac{\left(\frac{dX}{dT}\right)_0 - \frac{dX}{dT}}{1 - \left(\frac{dX}{dT}\right)_0 \frac{dX}{dT}} \quad (12)$$

Assuming that $\left(\frac{dX}{dT}\right)_0$ ranges from -1 to 1 and $1 > \frac{dX}{dT} > -1$, we see that the relative velocity approaches 1 or -1 for all $\frac{dX}{dT}$ as the horizon is approached since the horizon is at $t = \pm\infty$, such that $\left(\frac{dX}{dT}\right)_0 = 1$ there. Equation 12 is also constant along a given hyperbola (i.e it is independent of t) since it represents the relative velocity between the moving and rest frames. In fact, it is the $\frac{dX}{dT}$ we get when setting $t = 0$ in Equation 6 which makes sense because at $t = 0$, the Schwarzschild basis vectors and Kruskal-Szekeres basis vectors are aligned there, meaning that the X and T in $\left(\frac{dX}{dT}\right)_{rel}$ are pure spacelike and timelike basis vectors and thus the derivative gives a true velocity relative to the rest frame. This is in contrast to the general $\frac{dX}{dT}$ which is a derivative without a clear spacetime meaning since the X and T coordinates are mixtures of space and time everywhere else.

It is also notable that Equation 11 is undefined when $t = \infty$ because there $\left(\frac{dX}{dT}\right)_0 = 1$ and $\left(\frac{dX}{dT}\right)_{rel} = -1$ which gives us $\frac{dX}{dT} = \frac{-1+1}{-1+1} = \frac{0}{0}$. Thus, the full derivative is undefined at $t = \infty$.

We will now get an expression for the Lorentz boosts of frames in motion relative to the rest frame. First, we note that the reference frame shown in Figure 1 is the rest frame at $t = 0$. If we chose the rest frame at some $t \neq 0$, the T and X axes would be boosted relative to the $t = 0$ frame because the rest frame has a non zero velocity in Kruskal-Szekeres coordinates when $t \neq 0$. So we want to find an expression for the Lorentz boost that uses $\left(\frac{dX}{dT}\right)_{rel}$ since that velocity is the velocity of frames in motion relative to the rest frame, regardless of what the Kruskal-Szekeres velocity of the rest frame is.

We can solve for $\frac{dt}{d\tau}$ in Equation 1 as follows:

$$\frac{dt}{d\tau} = \frac{1}{\sqrt{\left(1 - \frac{r_s}{r}\right) \left(1 - \left(\frac{dr}{dt}\right)^2 \left(1 - \frac{r_s}{r}\right)^{-2}\right)}} \quad (13)$$

We get the time dilation for the rest frame by setting $\frac{dr}{dt} = 0$. If we define $\left(\frac{dt}{d\tau}\right)_0 \equiv \frac{1}{\sqrt{\left(1 - \frac{r_s}{r}\right)}}$, this is the time dilation caused only by the spacetime curvature at r (i.e. this is the pure gravitational time dilation of the rest observer). We can define the Lorentz boost of the moving frame relative to the rest frame by dividing $\frac{dt}{d\tau}$ in Equation 13 by the gravitational time dilation $\left(\frac{dt}{d\tau}\right)_0$ since we are only interested in the time dilation relative to the rest frame when considering Lorentz boosts:

$$\begin{aligned} \gamma &= \frac{\frac{dt}{d\tau}}{\left(\frac{dt}{d\tau}\right)_0} = \frac{1}{\sqrt{1 - \left(\frac{dr}{dt}\right)^2 \left(1 - \frac{r_s}{r}\right)^{-2}}} \\ &= \frac{1}{\sqrt{1 - \left(\frac{dX}{dT}\right)_{rel}^2}} \end{aligned} \quad (14)$$

The rapidity ω relative to the local rest observer in Kruskal-Szekeres coordinates is given by:

$$\omega = \tanh^{-1} \left(\left(\frac{dX}{dT} \right)_{rel} \right) \quad (15)$$

Finally, we can combine these to get the Lorentz factor as a function of rapidity:

$$\gamma = \frac{1}{\sqrt{1 - \tanh^2(\omega)}} \quad (16)$$

The Kruskal-Szekeres coordinate axes in Figure 1 are the spacelike and timelike bases of the spacetime in the rest frames at $t = 0$ because $\frac{dX}{dT} = 0$ for the rest frames when $t = 0$. So $\left(\frac{dX}{dT}\right)_{rel}$ is the velocity of the falling frame as seen from the rest frame. But a falling frame will have an increasing velocity relative to the rest observers, and therefore, their reference frames will be Lorentz boosted relative to the rest frame per Equation 14. Figure 2 shows three snapshots of boosted falling frames that started falling from infinity with the frame's r coordinate (the r the frame had fallen to when the boost is being depicted) labelled below each snapshot.

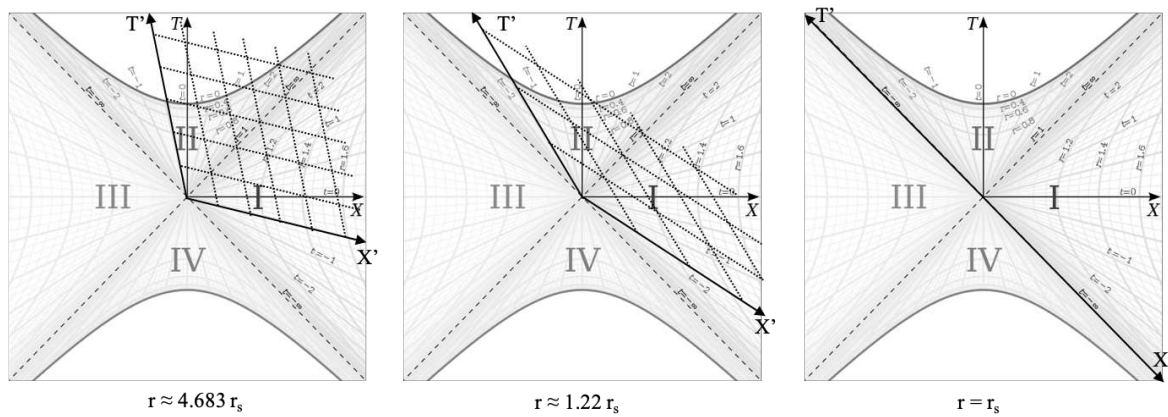


Figure 2. Lorentz Boosted Frames During Freefall

In this figure, we can see that the basis vectors of the boosted frames are rotated relative to the rest frame (the X' and T' axes represent the boosted frames).

From this, we can also get a sense of length contraction in the falling frame. Firstly, we must note that the dX term of the metric really should be dR since it represents a change in the radial position of a particle. This means the Lorentz boost the falling frame experiences when it falls is radial in all directions, with the origin of the frame at the horizon (it is the radial $\partial_X = \partial_R$ basis vector that rotates in Figure 2). The planar surfaces perpendicular to a Cartesian coordinate axis in the Minkowski metric become spherical surfaces centered on the metric source in the Schwarzschild metric. So when we talk about length contraction in a radially falling frame, we are saying that circumferences around the source of the metric are length contracted in that frame and remain circular. This radial contraction is necessary for all inertial observers to see the spacetime as spherically symmetric. If the length contraction was dependant on the direction of the radial fall, then inertial observers would disagree on the spherical symmetry of the metric.

We can see the length contraction effect in Kruskal-Szekeres coordinates by looking at the X distance from the horizon to some radius r along a line of constant T for two different cases where the observers started falling from a different radius in each case such that when when we look at the frame of each observer at some time after they started falling, the Lorentz factor and rapidity have different values for each case.

In the above figure, the left frame has a lower radial velocity and therefore a lower rapidity ($\omega = -0.25$ in this case) relative to the right frame, which has a rapidity of $\omega = -0.75$. We chose the same point in both frames for comparison to look at its distance from the event horizon in both frames. By comparing the dark lines in each picture, which represent the distance from the horizon to some r (the same r in both cases) measured in X' at constant T' in each frame, we clearly see that this distance is shorter in the frame on the right compared to the frame on the left.

We can calculate the actual ratio of the lengths in the two frames given the length contraction equation $X = \frac{X_0}{\gamma}$. The ratio of the lengths of the lines on the left (X_L) and right (X_R) sides of Figure 3 will be a ratio of Lorentz factors. We can see from the figure, that $\omega_L = -0.5$ and $\omega_R = -1.5$. Using Equation 16, we can solve for the ratio of the lengths in the falling frames as:

$$\frac{X_L}{X_R} = \frac{\gamma_R}{\gamma_L} = \sqrt{\frac{1 - \tanh^2(-0.25)}{1 - \tanh^2(-0.75)}} \approx 1.26 \quad (17)$$

Note that we would get the same result regardless of which point on the r hyperbola we draw the line to, as long as we use the same point in all frames being compared and draw the lines to the horizon along a line of constant T in each frame.

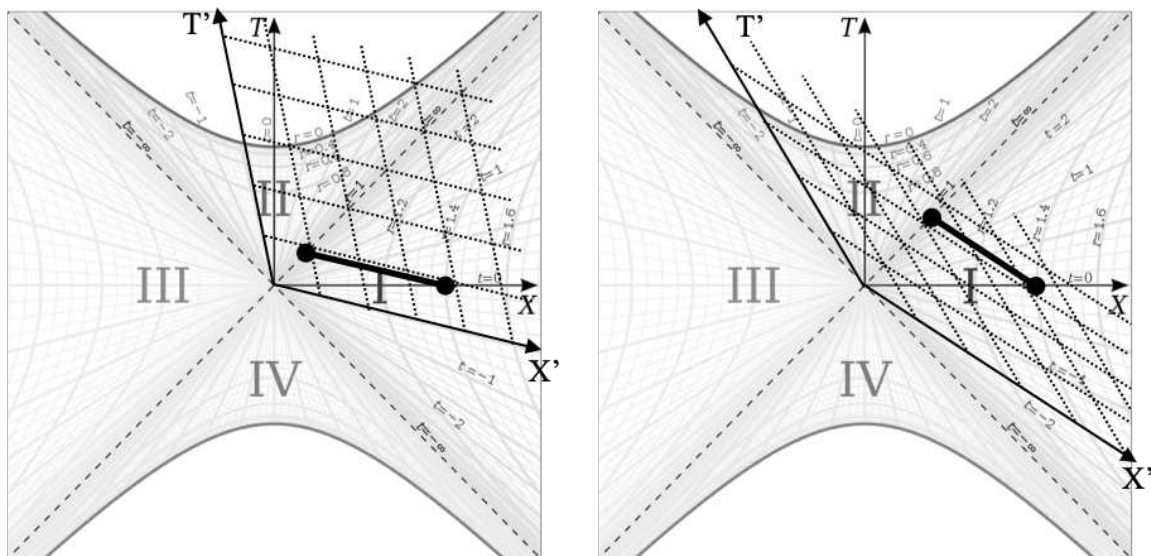


Figure 3. Length Contraction in the Falling Frame

As the rapidity increases further, we can see that this line will tend toward a null geodesic as the horizon is approached indicating that the spacetime contracts fully to the horizon in the falling frame, which is consistent with the argument that the falling frame becomes light-like at the horizon.

The contraction of the r coordinate in these frames relative to the rest frame can be calculated by plugging the contracted X length into Equation 2 and solving for r . By calculating the contracted r coordinate, we can calculate the contracted circumferences around the metric source in the falling frame and we can see from the above analysis that these circumferences will contract to zero when the frame reaches the horizon.

Given the length contraction observed, the observer should also see the volume of the source contract in the falling frame. Applying the length contraction equation to the volume of the source:

$$V' = \frac{V}{\gamma^3} = \frac{4\pi r_s^3}{3\gamma^3} \quad (18)$$

Where r_s is the Schwarzschild radius. The mass of the source is related to its Schwarzschild radius by $M = \frac{r_s c^2}{2G}$. If we assume the mass of the source is within the Schwarzschild radius, the density of the source in the falling frame is given by

$$\begin{aligned} \rho &= \frac{M}{V'} \\ &= \frac{3c^2}{8\pi G r_s^2} \gamma^3 \end{aligned} \quad (19)$$

So in the falling frame, γ goes to infinity as the horizon is approached such that the density there also goes to infinity. This shows us that due to the length contraction, there is no space beyond the event horizon in the falling frame, indicating that the event horizon is the end point of gravitational collapse. At the horizon, the falling frame will see the entire Universe radially length contracted to the horizon as well due to length contraction. This is reflected in the rest frame by the fact that all hyperbolas intersect with the horizon when $t = T = X = \infty$, which is the horizon itself. We see therefore that the Kruskal-Szekeres coordinates represent the spacetime in the frame of the source which is an infinitely dense point at $r = 1$. This point looks like a surface to a distant observer, but is length contracted to a point when the horizon is approached.

What has been demonstrated here is that the $T = X = 0$ point on the Kruskal-Szekeres chart represents the source of the metric. In fact, all the points on the $T = \pm X$ lines are the same event

since they all have the same spatial coordinate $r = r_s$ and the points on those lines are connected by null geodesics. So if two points on the chart have the same spatial location and are separated by zero proper distance, then they must be the same event. So, in a sense, X marks the spot of the metric source in the Kruskal-Szekeres coordinate chart.

What the Kruskal-Szekeres coordinates tell us is that the Schwarzschild metric is not only spherically symmetric, but also hyperbolically symmetric (the hyperbolic symmetry is manifest in the external metric as time-independence). As will be discussed, the hyperbolic symmetry manifests as homogeneous space in the context of the external metric. The metric symmetries will be further discussed in Section 4.

This leaves us with two important questions. The first is what do the other three regions of the chart represent. The second is what is the $r = 0$ curvature singularity and what happens there if it is not the source of the metric. These questions are the focus of the remainder of the paper.

4. Symmetries of the Schwarzschild Geometry

Having discussed the geometry of the external metric, let us turn to the internal metric (Region II in Figure 1). The internal form of metric can be expressed as:

$$d\tau^2 = - \left(1 - \frac{u}{r}\right) dt^2 + \frac{1}{1 - \frac{u}{r}} dr^2 - r^2 d\Omega^2 \quad (20)$$

Equation 20 is the internal metric and for the rest of the paper it is important to remember that when discussing the internal metric, *t is the spacelike coordinate and r is the timelike coordinate*. To help distinguish between the r , t , τ , and Ω coordinates in the internal and external metrics, *from this point forward, we will denote the external metric with primed coordinates: r' , t' , τ' , and Ω'* . So r refers to the internal coordinate and r' refers to the external coordinate. This delineation will be important in later sections.

The internal metric is currently believed to describe the interior of a Black Hole. But consider the case of a spherically-symmetric vacuum surrounded by a spherically-symmetrically distributed infinite amount of mass. This would be a spacetime surrounded by a shell with an infinite Schwarzschild radius (because the mass of the shell is infinite). Since this is a spherically symmetric vacuum, it must be described by the Schwarzschild metric. This is also the description of spherically-symmetric vacua in our Universe, since the surrounding Universe is effectively a shell of infinite mass (every region of the Universe is light-like connected to the Big Bang in all directions, which acts as a shell of infinite mass/Schwarzschild radius). Therefore, the internal metric describes the spacetime of the pockets of empty space in the Universe. The constant u in the internal metric is a time constant whose value in years will be later derived from cosmological data. Choosing a value for this constant amounts to choosing the units of time for analysis. This metric is essentially the Minkowski metric with a variable speed of light, which can also be interpreted as an expanding or collapsing space.

So the Schwarzschild metric describes the curved spacetime caused by an infinitely dense shell from two perspectives:

- The external metric describes the spacetime around an infinitely dense shell of finite mass and radius in the frame of an observer infinitely far away from the shell
- The internal metric describes the spacetime inside an infinitely dense shell located at infinity in the frame of an observer at rest inside the shell. In the case of the Universe, the shell would be the entire Universe at time $r = u$ (as will be shown, the scale factor is zero there and therefore we have infinite coordinate density).

Figure 1 shows the Kruskal-Szekeres coordinate chart for both the internal and external metrics where light travels on 45 degree lines on the chart. This will help illustrate the above points more clearly.

On this diagram, the $T = \pm X$ lines represent the infinitely dense shells in both scenarios. We can see that at $r = r_s = u$ (the 'Horizon'), both metrics are the same. The origin $T = X = 0$ location/time

describes an infinitely dense point in space for the external solution for all time and a time at which all infinite space is contracted for the external solution. The $T = \pm X$ lines are light-like because light cannot escape an infinitely dense region of space, regardless of the mass (i.e. the external observer cannot receive light emitted from the Schwarzschild radius and the internal observer cannot receive light from the time when space was infinitely contracted). The different quadrants of Figure 1 will be examined in Section 10. We can also see in Figure 1 that for the internal metric, the horizon is located at $t = \infty$, meaning the Schwarzschild radius and therefore mass of the shell is infinite (because t is the spacelike coordinate). Thus, it is clear from the geometry that the source masses of the Schwarzschild metric are not concentrated at $r = 0$ (which is currently assumed and accepted by most physicists today, but is not anywhere mathematically implied or demanded in the derivation of the Schwarzschild metric), but rather at the event horizon itself.

So the internal solution describes a spherically symmetric vacuum surrounded by a horizon which, from the perspective of an observer at some r between the horizon and $r = 0$, surrounds the vacuum infinitely far away in space and at some finite time in the past. And from the perspective of that observer, this horizon, which looks like a surrounding sphere, is a time where space is infinitely dense. A spacetime fitting this description would be any empty space in the Universe whose surrounding mass is spherically symmetric. Voids in the cosmic web would be an example of such a spacetime, and the horizon of the metric in this case would be the Big Bang, which is an event at some finite time in the past that surrounds all points in the Universe which has an infinite density. And an observer in the present Universe can never reach the Big Bang, no matter how far they travel through space, which is in alignment with the fact that the surface, from the perspective of a present observer, is infinitely far away from them in space. So we might think of the expanding Universe as baking bread where the air pockets that expand as the bread bakes give the bread a web-like structure over time, where the bread itself would be analogous to the cosmic filaments of matter in the Universe.

Therefore, the Big Bang looks like an infinitely dense shell (viewed from the inside) at times later than the Big Bang, but looks like an infinitely dense point (because the proper distance goes to zero regardless of coordinate distance at that time) in the frame of an observer in the Universe as the Universe approaches that time (we will show that the scale factor at $r = u$ is 0 in Section 6). In other words, both the internal and external metrics look the same in the frame of an observer approaching the source, which is to be expected since they have the same mathematical description there.

Now we must show that the space in the internal metric is isotropic and homogeneous. The equation for a 2D hyperboloid surface embedded in three dimensions is given by:

$$\frac{x^2}{a^2} + \frac{y^2}{b^2} - \frac{z^2}{c^2} = \pm 1 \quad (21)$$

For our purposes, we will be considering the special case where $a = b = c$, which gives the one and two sheeted hyperboloids of revolution. Next, we note the following relationship with regards to the Kruskal coordinates:

$$X^2 - T^2 = \left(\frac{r}{u} - 1\right) e^{\frac{r}{u}} \quad (22)$$

Equation 22 is only for one dimension of space, but we know that the metric is spherically symmetric and can therefore extend Equation 22 to 2 spatial dimensions by simply adding a Y coordinate to get an equation that matches the form of Equation 21 where $a^2 = b^2 = c^2 = \left(\frac{r}{u} - 1\right) e^{\frac{r}{u}} \equiv \rho^2$:

$$X^2 + Y^2 - T^2 = \rho^2 \quad (23)$$

Equation 23 describes 2D hyperboloid surfaces for a given r where the external metric has positive ρ^2 and the internal metric has negative ρ^2 . This means that the external metric describes a 1-sheet hyperboloid while the internal metric describes a 2-sheeted hyperboloid.

We will for now focus on regions I and II from Figure 1, where region I captures the external metric and region II captures the internal metric. If we choose some constant value of $r = r_0$ in each region and plot Equation 23 for each region, we get the surfaces shown in Figure 4.

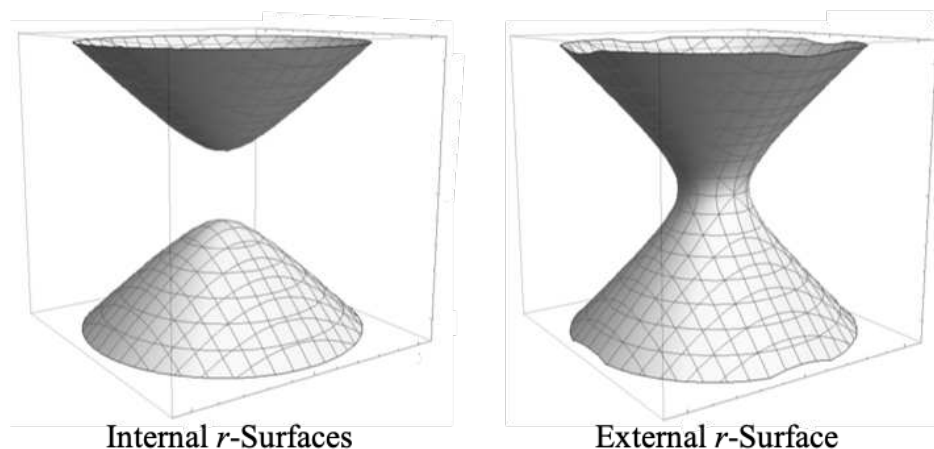


Figure 4. 2D Surfaces of Constant r for Internal and External Metrics

In the internal case where we have two separate sheets, we will only focus on the top sheet for now. The meaning of the bottom sheet will be discussed in Section 10. In the external metric, the sheet represents an equatorial circle of space around the central body at all times. This circle is on a plane with a normal at the center and pointed vertically in Figure 4. If we then consider circles on all planes whose normals are at different angles relative to the normal of the plane we are currently visualizing, we get a 2D spherical surface representing the space surrounding the central body at constant r .

Light cones in Figure 4 are oriented vertically and light travels on 45 degree lines. If we consider the right side of Figure 4, representing the external metric, choose any point on the surface and project a past and future light cone out of that point (this will just be a vertical cone centered at that point). We see that the external metric is anisotropic and inhomogeneous because the surface is asymmetric relative to the surface left and right as well as into and out of the page. But the light cone is symmetric vertically relative to the surface. We can see this because we are allowed to circularly and/or hyperbolically rotate any point to a point at the throat of the surface and the space will remain unchanged. This is because the metric is spherically symmetric (representing circular rotations) and static (representing hyperbolic rotations). It becomes clear that the cone is vertically symmetric relative to the surface at the throat since both the cone and surface are vertically symmetric in a plane parallel to the throat. So any point we choose to start with can be moved to the throat of the surface and we see that the cone is vertically symmetric relative to the surface when we move a point there.

Now consider the top sheet on the left side of Figure 4 representing the internal metric. Again choose any point on the surface and project a past and future light cone vertically from that point. Just like in the case of the external metric, we can move that point anywhere on the surface to the apex of the surface by hyperbolically and/or circularly rotating the point there (and the space will remain unchanged). When the point is rotated to the apex, we see then that the light cone is symmetric relative to the surface left and right and into and out of the page. This symmetry means the internal metric is isotropic and homogeneous. The cone is not vertically symmetric relative to the surface, however, and that reflects the fact that the internal metric is not static.

The above arguments tell us something important about the Schwarzschild metric. When the metric is derived from Einstein's field equations, it is usually done from the perspective of the external metric. In the derivation, we assume spherical symmetry and a static spacetime. It is notable that in spite of the static assumption, we still get an internal metric that is non-static. This is because the static assumption for the external metric is actually an implicit assumption of hyperbolic symmetry. Therefore, we can more correctly state that the Schwarzschild metric is the vacuum solution to

Einstein's field equations that is both spherically and hyperbolically symmetric. This hyperbolic symmetry manifests itself as a static metric when the time coordinate is hyperbolic (the external metric) and an isotropic and homogeneous metric when the space coordinate is hyperbolic (the internal metric).

We can further extend this to three spatial dimensions by adding a Z^2 term to Equation 23, and given the spherical symmetry we can define $R^2 \equiv X^2 + Y^2 + Z^2$ and change Equation 22 to

$$R^2 - T^2 = \rho^2 \quad (24)$$

In this formulation, we put ourselves at $R = 0$ and the circles on the surfaces in Figure 4 will become spheres that are isotropic and homogeneous in space and inhomogeneous in time, which is consistent with the Cosmological Principle.

Let us examine the Killing vectors for the geometry on a surface of constant r in the internal metric. In the 1D spatial representation of the metric in quadrant II of Figure 1, we see that the spacelike coordinate t has positive and negative values. Given the spherical symmetry of the metric, we can construct a Cartesian basis in t for the metric at fixed time r as follows:

We know that ∂_t is a Killing vector of the spacetime and the X, Y, Z labels in Figure 5 represent the 3 spatial directions in Kruskal coordinates. The perpendicular hyperbolas shown on the sheets on the left side of Figure 4 represent the $\partial_{t,X}$ and $\partial_{t,Y}$ coordinates of Figure 5. So we see that we can construct a Cartesian basis for the 3D space of the internal metric out of Killing vectors and therefore the 3D space of the metric must be homogeneous and isotropic at a given time r . So all motion through space in the internal metric can be described as motion in the basis depicted in Figure 5 (i.e. even circular motion involves changes in location t).

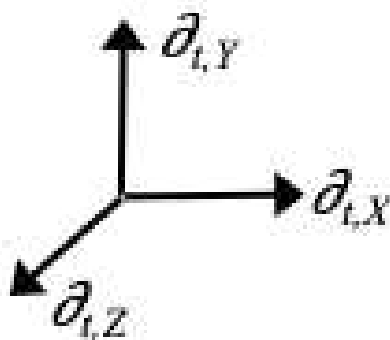


Figure 5. Cartesian Killing/Basis Vectors on a Surface of Constant r

In the external metric, the t Killing vector runs in the T direction of the Kruskal coordinates and so it has more of a radial characteristic. Therefore, in the external metric, $\partial_{t,T}$ can be seen as pointing in all directions at fixed r . The circles on the sheets on the right side of Figure 4 are circles of constant time t . Figure 6 shows these contours on a plane with the Killing/Basis vectors $\partial_{t,T}$ plotted on the contours.

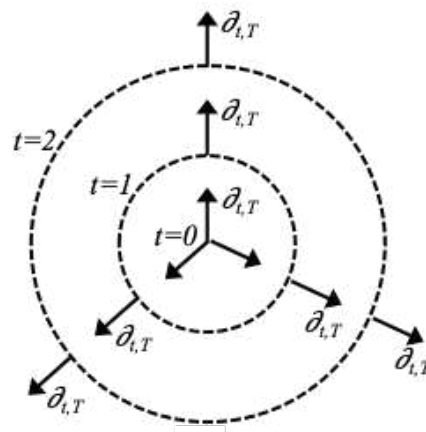


Figure 6. Radial Killing/Basis Vectors on a Surface of Constant r

It is important to note here that in the external metric, the angular term $d\Omega$ describes the translation of a reference frame along a curvilinear path, whereas in the internal metric, the term describes the precession of a reference frame about an axis of time. This implies that the angular term in the internal metric is describing a spin about the time axis (r), which is discussed in Section 5. Curvilinear motion through space is also discussed in Section 9.

From this analysis, we can see that the Kruskal coordinates are extrinsic coordinates, allowing us to view the full geometry from 'the outside', as opposed to the Schwarzschild coordinates which are intrinsic. The extrinsic nature of the Kruskal coordinates is what makes the event horizon seem like a non-special location that is traversable without issue even though in actuality, that location/time represents a hard boundary of infinite coordinate density (the curvature there is not infinite, but the geometry is discontinuous there and that discontinuity is obscured in the extrinsic basis). This is the 4D equivalent of looking at the surface of a sphere in 3D using an extrinsic Cartesian basis (in fact, if we plotted a surface in the X, Y, Z Kruskal coordinates at fixed r instead of T, X, Y as shown in Figure 4, we would see spherical surfaces plotted in a Cartesian basis). Note that if we plotted one such sphere in the Kruskal X, Y, Z basis, we would see that the surface shrinks to a point when $r = u$, supporting the argument that the horizon is a point of infinite coordinate density.

To show this, we first note the definition of the Kruskal T coordinate in terms of the Schwarzschild coordinates for the internal metric:

$$T^2 = \left(1 - \frac{r}{u}\right) e^{\frac{r}{u}} \cosh^2\left(\frac{t}{2u}\right) \quad (25)$$

If we substitute Equation 25 into Equation 24 and solve for R we get:

$$R = \sqrt{\left(1 - \frac{r}{u}\right) e^{\frac{r}{u}} \sinh^2\left(\frac{t}{2u}\right)} \quad (26)$$

Therefore, we see that as r approaches u , R goes to zero for all t .

Now imagine we are situated at some point in empty space in the Universe facing in some direction. There is a plane of infinite space at the present time perpendicular to the direction we are facing. This plane is the hyperbolic sheet depicted on the left side of Figure 4 where we are situated at the apex of the sheet. So the direction we are facing is the normal vector to this sheet (with the vector origin at the apex of the sheet) and just like in the external case, there are similar planes constructed from normals at all different angles to the direction we chose to face and when we put all of these together, we get an infinite 3D space at the present time.

But the points on this collection of sheets at r_0 are spacelike to us because they all exist at the same time as us and we can only see points on past sheets whose light has had time to reach us. Light

paths in Figure 1 are lines at 45 degrees and light cones in Figure 4 are oriented vertically where the beginning of the Universe is at the origin between the two sheets and time moves forward as the top sheet moves up the diagram vertically. So we can construct an image of what a 2D slice of the Universe would look like to us in this geometry with our position at the center. Figure 7 shows the present sheet (r_0) where we are positioned in space at the apex of the sheet. We then show a cross section of that sheet on the Kruskal-Szekeres coordinate chart with the past light cone shown (dashed lines at 45 degrees emanating from $t = 0$ at r_0). That light cone intersects past sheets of constant $r > r_0$ (past sheets not shown in the top left of Figure 7 but are represented by the hyperbolas the dashed lines intersect in the top right of the figure) and these intersections are projected onto the plane at the origin to give us a 2D image of our past light cone of the Universe. The density of the coordinates at different radii (and therefore times) is depicted with the shading inside the projection.

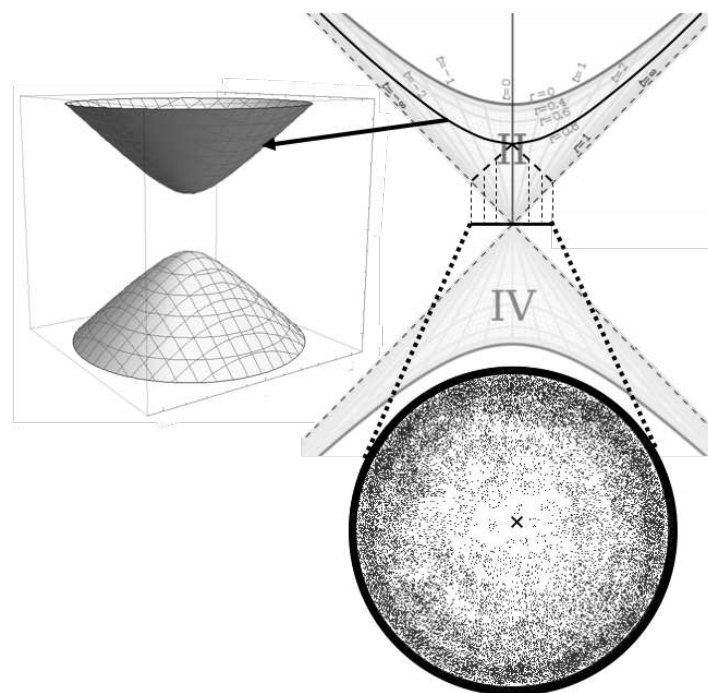


Figure 7. Projection of the Past Light Cone on a Flat Plane

Despite the hyperbolic nature of the spacelike planes, space still looks flat from our perspective because our past light cone intersects past surfaces as circular cross-sections. As we can see in the lower projection in Figure 7, concentric circles around the center of the projection (marked with 'x') are circles of constant distance and time from us. So we see that as we look further away in space and back in time, the Universe becomes more dense until at the beginning of the Universe, which corresponds to an infinite distance and finite time from us, the Universe is infinitely dense. This is in line with our current observations of the Universe.

5. The Angular Term $r^2 d\Omega^2$

To understand the angular term of the internal metric, let us first think about the external metric in a reference frame attached to an observer in the gravitational field of a star. In this frame, if the observer is in circular orbit around the star, then the star will appear to revolve around the observer. But the star will also appear to revolve around the observer if the observer is just spinning in place. In order to distinguish between these two cases, we need a gyroscope.

We start by drawing a line between the observer and the star and orient the axis of the gyroscope along this line. In the frame of the observer, if the gyroscope maintains its orientation along this line as the star revolves around the observer, then they know they are just spinning in place and not actually

orbiting the star. If however they see that the angle between the gyroscope axis and connecting line changes as the star revolves around the observer, then they know they are in orbit around the star and their angular velocity as described by the angular term in Equation 1 will be the rate at which the angle between the gyroscope axis and connecting line changes. So the angle of the external metric describes the angle between a gyroscope axis and a line connecting the observer's reference frame to the center of the source body of the metric.

For the internal metric, there is no central body like the star that can be referenced as the source of the metric. Instead, we must use the distant surrounding Universe as a reference, with the Cosmic Microwave Background being an optimal reference in this case. Just like in the external case, we can draw a line from the observer to some point on the CMB and orient the gyroscope along that line. As we move through empty space, the change in angle between the gyroscope axis and the connecting line will be the change in angle $d\Omega$ in Equation 20, representing a change in the orientation of the reference frame. In a Newtonian Universe, this angle would never change because even if we moved around a curvilinear path through space, the gyroscope would remain fixed in its orientation. But in Special Relativity, there is a kinematic effect known as Thomas Precession in which the orientation of the gyroscope will change as a result of an acceleration being applied to the observer at an angle to the observer's current velocity. The Thomas Precession is given by:

$$\vec{\omega}_T = \frac{1}{c^2} \left(\frac{\gamma^2}{\gamma + 1} \right) \vec{a} \times \vec{v} \quad (27)$$

Where

$$\gamma = \frac{1}{\sqrt{1 - \frac{v^2}{c^2}}} \quad (28)$$

At non-relativistic speeds, this precession is very small, essentially zero at human scales. Also note that we do not include dynamical relativistic precession effects such as geodetic precession and frame dragging in this because those effects are accounted for by the metrics describing the curved spacetime that causes them. We discuss how to find the total proper time of a worldline resulting from the combined metrics in Section 13. We can think of this kinematic precession as the 'spin' of an object since it is an intrinsic rotation of the object's reference frame.

As will be discussed in Section 9, $\frac{dt}{dr}$ is related to the magnitude of the CMB dipole that would be seen when moving through space. In terms of curvilinear motion, $\frac{dt}{dr}$ will always represent the tangential velocity to the observer's path. Furthermore, the combination of the CMB dipole's magnitude as well as the angular velocity of the dipole as it moves across the CMB will give us the acceleration normal to the path at each point. Noting that the centripetal acceleration of a body moving with tangential velocity v and angular velocity ω can be expressed as $a = \omega v$, we can get an alternate expression for the Thomas Precession as follows:

$$\vec{\omega}_T = \vec{\omega}_D \left(\frac{\gamma^2}{\gamma + 1} \right) \left(\frac{1}{c} \frac{dt}{dr} \right)^2 \quad (29)$$

Where $\vec{\omega}_D$ is the angular velocity of the CMB dipole as it moves over the CMB and $\frac{dt}{dr}$ is the tangential velocity, which is related to the magnitude of the CMB dipole. If we create a basis for the observer's reference frame by aligning gyroscopes along the $\partial_{t,X}$, $\partial_{t,Y}$, and $\partial_{t,Z}$ directions, then we can define the angles θ and ϕ in that basis which describe the general motion of the dipole over the CMB. With those, we can express Equation 29 in terms of θ and ϕ as:

$$\omega_\Omega = (\omega_{D,\theta} + \omega_{D,\phi} \sin \theta) \left(\frac{\gamma^2}{\gamma + 1} \right) \left(\frac{1}{c} \frac{dt}{dr} \right)^2 \quad (30)$$

Therefore, Equation 30 tells us how the orientation of the observer's reference frame changes at each instant while the observer is in motion, giving us the magnitude of $\frac{d\Omega}{dr} = \omega_\Omega$ for the frame at each instant. This change in orientation manifests itself in the frame of the observer as a rotation of the surrounding Universe around the basis defined by the aforementioned gyroscopes. An important thing to note here is that at modest speeds ($\frac{dt}{dr} \ll c$), the rotation of the reference frame's orientation (which is what the internal metric describes), is much lower than the rotation of the CMB dipole such that if the dipole makes a 2π rotation in a given amount of time, the actual angle of rotation in the metric will be much lower than 2π over the same period of time. We can further simplify Equation 30 by noting that $\left(\frac{1}{c} \frac{dt}{dr}\right)^2 = \frac{\gamma^2 - 1}{\gamma^2} = \frac{(\gamma + 1)(\gamma - 1)}{\gamma^2}$, giving us:

$$\omega_\Omega = (\omega_{D,\theta} + \omega_{D,\phi} \sin \theta) (\gamma - 1) \quad (31)$$

But from the metric, it is clear that there can still be precession of the reference frame, even if there is no centripital acceleration through space (there are timelike paths where $dt = 0$ in the metric). An observer moving in a straight line with a precessing inertial frame would see the CMB dipole angle fixed relative to the gyroscope basis and the entire Universe would appear to rotate around the gyroscopes. The same would be true for a co-moving observer with the difference being that there would be no dipole visible on the CMB. The inertial rotation could also be deduced without the dipole or gyroscopes because the reference frame precession for an inertial observer would create a quadrupole on the CMB in the observer's frame. The features of this quadrupole would contain the information needed to determine the $d\Omega$ term of the metric for the inertial observer with a precessing frame.

Going back to the two-sheeted hyperboloid in Figure 4, we can keep our observer's frame fixed at the apex of the sheet and describe this precession as the sheet revolving around the apex (i.e. from the observer's frame, it appears the Universe is revolving around them). Likewise, we can describe motion in the t dimension by again keeping the observer fixed at the apex and hyperbolically rotating the sheets under the observer in the direction of travel. Given these interpretations of the motion in t and Ω , it is notable that if an object had some intrinsic spin already and started moving in t , the object would move on a curved trajectory analogous to a charged particle moving in a magnetic field.

In the frame of an observer with this intrinsic spin, they see the entire Universe rotating around their inertial frame as they move in a straight line relative to their basis. But from an external frame, the particle with spin will move on a curved trajectory under the influence of a fictitious cosmological Coriolis force (the momentum vector of the particle rotates without an external force being applied as a result of the precession of the inertial frame). This effect could be related to the Dark Matter effects observed in galaxy rotation curves. If when the galaxies formed, the rotation of the gases was high enough, they could have gained enough of this spin such that as the stars that subsequently formed from the gas migrated out from the center, they would experience this Coriolis acceleration and maintain an orbit about the galactic center with greater tangential velocity than expected. At the present time, however, this is mere conjecture and would require further study to verify.

The path of light should also be affected by the angular term of the metric. When light is gravitationally lensed, its momentum vector changes direction, so from the perspective of the light, the Universe has rotated around it. We can see the precise behaviour of lensed light by looking at the geodesic equation for angular motion [1] (we will examine the case for planar rotation where $\theta = \frac{\pi}{2}$).

$$\frac{d^2\theta}{d\lambda^2} = -\frac{2}{r} \frac{d\theta}{d\lambda} \frac{dr}{d\lambda} \quad (32)$$

For light, we will use $\lambda = r$. If we consider light lensed by a galaxy, as the light passes the galaxy at some coordinate time r_0 , it will have some angular velocity $\dot{\theta}_0$ and initial angle θ_0 as it leaves the galaxy. It is currently assumed that the light then continues along a straight line as it leaves the gravitational field, but as we shall see, this is not the case. The θ_0 would be the angle caused only by the gravitational

lensing, without any additional effects from the cosmological model (i.e. the angle we would expect when only taking into account the mass of the galaxy). Given these initial conditions, the solution to Equation 32 is:

$$\theta(r) = \theta_0 + \dot{\theta}_0 r_0 \left(1 - \frac{r_0}{r}\right) \quad (33)$$

During expansion, both the bracketed expression and $\dot{\theta}_0$ will always be negative (because dr is negative and $r_0 > r$) such that the second term is always positive. Therefore, during expansion, the observed lensing angle will be increased by the amount $\dot{\theta}_0 r_0 \left(1 - \frac{r_0}{r}\right)$ as a result of this effect (where r is the coordinate time at which the light is observed). Furthermore, since $\frac{d\Omega}{dr}$ for the light increases over time, the $\frac{dt}{dr}$ will correspondingly decrease as well and the result of this is that the increase in lensing angle over time will also result in a redshift of the light relative to unlensed light.

We see that the 'excess angle' is dependant on the lensing rate $\dot{\theta}_0$. So if we consider two cases where in one case, the light is gently lensed over a large distance/time by some angle θ_0 and in the other case, light is lensed by a more dense mass the same θ_0 , the lensing rate $\dot{\theta}_0$ would be higher in the second case relative to the first. So even though the pure gravitational lensing angle θ_0 would be the same in both cases, the observed angle would be greater in the second case because the lensing rate $\dot{\theta}_0$ would be greater in that case.

Note that Equation 32 would also apply to the precession of the inertial frames of the stars in the galaxies.

6. The Scale Factor

Expressions for the proper time interval along lines of constant t and Ω and the proper distance interval along hyperbolas of constant r and Ω from Equation 20 are:

$$\frac{ds}{dt} = \pm \sqrt{\frac{u-r}{r}} = \pm a \quad (34)$$

$$\frac{d\tau}{dr} = \pm \sqrt{\frac{r}{u-r}} = \pm \frac{1}{a} \quad (35)$$

And the coordinate speed of light is given by:

$$\left(\frac{dt}{dr}\right)_{light} = \pm \frac{r}{u-r} = \pm \frac{1}{a^2} \quad (36)$$

Where a is the scale factor (because t is the spatial coordinate and r is the time coordinate and therefore Equation 34 describes how the proper distance between two points separated by coordinate distance dt evolves over time). First we should notice that none of the three equations depend on the t coordinate. This is good because the t coordinate marks the position of other galaxies relative to ours. Since all galaxies are freefalling in time inertially, the particular position of any one galaxy should not matter. The proper temporal velocity, proper distance, and coordinate speed of light only depend on the cosmological time r .

A plot of the scale factor vs. r (with $u = 1$) is given in Figure 8 below:

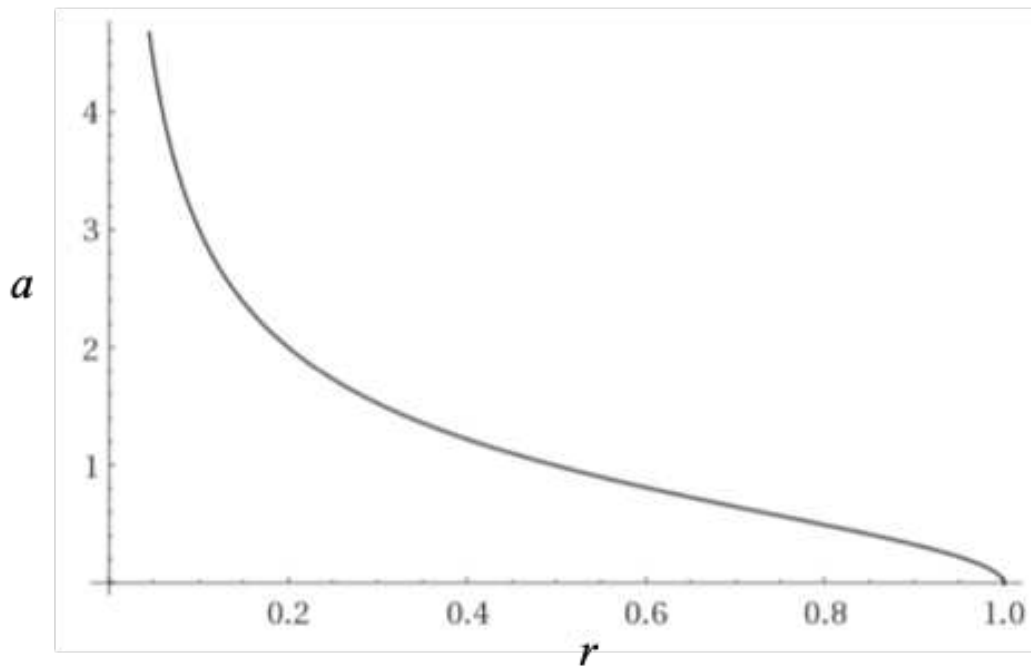


Figure 8. Scale Factor vs. r for $u = 1$

7. The Co-Moving Observer

Let us take a co-moving observer somewhere in the Universe we label as $t = 0$ as the origin of an inertial reference frame. We can draw a line through the center of the reference frame that extends infinitely in both directions radially outward. This line will correspond to fixed angular coordinates (Ω). There are infinitely many such lines, but since we have an isotropic, spherically symmetric Universe, we only need to analyze this model along one of these lines, and the result will be the same for any line.

We must determine the paths of co-moving observers ($dt = d\Omega = 0$) in the spacetime. For this we need the geodesic equations for the internal Schwarzschild metric [1] given in Equation 20. In these equations u represents a time constant (in Figure 1, the value of u is 1). The following equations are the geodesic equations of the internal metric for t and r ($0 \leq r \leq u$) for $d\Omega = 0$:

$$\frac{d^2 t}{d\tau^2} = \frac{u}{r(u-r)} \frac{dr}{d\tau} \frac{dt}{d\tau} \quad (37)$$

$$\frac{d^2 r}{d\tau^2} = \frac{u}{2r^2} \quad (38)$$

Looking at points $0 < r < u$, then by inspection of Equation 37 it is clear that an inertial observer at rest at t will remain at rest at t ($\frac{d^2 t}{d\tau^2} = 0$ if $\frac{dt}{d\tau} = 0$).

Let us next demonstrate how the internal metric fits with existing cosmological data and calculate various cosmological parameters using that data.

8. Calculation of Cosmological Parameters

In order to compare this model to cosmological data, we must solve for u and find our current position in time (r_0) in the model. Reference [4] gives us transition redshift values ranging from $z_t = 0.337$ to $z_t = 0.89$, depending on the model used. We can use the expression for the scale factor in

Equation 34 to get the expression for cosmological redshift from some emitter at r measured by an observer at r_0 [1]:

$$1 + z = \frac{a_0}{a} = \sqrt{\frac{r(u - r_0)}{r_0(u - r)}} \quad (39)$$

Furthermore, the deceleration parameter is given by:

$$q = \frac{\ddot{a}a}{\dot{a}^2} = \frac{4r}{u} - 3 \quad (40)$$

By setting Equation 40 equal to zero, we find that the scale factor at the transition from decelerating to accelerating expansion a_t is:

$$a_t = \sqrt{\frac{4}{3} - 1} = \frac{1}{\sqrt{3}} \quad (41)$$

Using Equations 39, 41, and the transition redshift estimate, we can get an expression for the present scale factor:

$$a_0 = a_t(1 + z_t) = \frac{1 + z_t}{\sqrt{3}} \quad (42)$$

Next, we find expressions for u and our current radius r_0 by noting that the Universe has been found to be roughly 13.8 billion years old. Therefore, we can set $\alpha_{r_0} \equiv u - r_0 = 13.8$ and use Equations 34 and 42 to obtain the following for u and r_0 :

$$r_0 = \frac{u - r_0}{a_0^2} = \frac{\alpha_{r_0}}{a_0^2} = \frac{3\alpha_{r_0}}{(1 + z_t)^2} \quad (43)$$

$$u = r_0 + \alpha_{r_0} = \alpha_{r_0} \left(\frac{3}{(1 + z_t)^2} + 1 \right) \quad (44)$$

Next we compute the CMB scale factor (a_{CMB}) and coordinate time (r_{CMB}) in this model where the redshift of the CMB (z_{CMB}) is currently measured to be 1100:

$$a_{CMB} = \frac{a_0}{1 + z_{CMB}} \quad (45)$$

$$r_{CMB} = \frac{u}{1 + a_{CMB}^2} \quad (46)$$

We can next derive the Hubble parameter equation using the scale factor. The Hubble parameter is given by (in units of $(Gy)^{-1}$):

$$H = \frac{\dot{a}}{a} = \frac{u}{2r(u - r)} \quad (47)$$

Table 1 below gives the values of u , r_0 , H_0 , a_0 , q_0 , a_{CMB} , r_{CMB} , and q_{CMB} given the upper and lower bounds of z_t from [4] as well as the average of the upper and lower bound values and assuming $\alpha_{r_0} = 13.8$. All times are in Gy and H_0 is in $(km/s)/Mpc$.

Table 1. Limiting Cosmological Parameter Values Based on z_t Measurement and a 13.8 Gy Age of the Universe

z_t	α_{r_0}	u	r_0	H_0	a_0	q_0	a_{CMB}	r_{CMB}	q_{CMB}
0.337	13.8	37.0	23.2	56.6	0.77	-0.49	0.0007	36.95	0.99
0.614	13.8	29.7	15.9	66.2	0.93	-0.86	0.0008	29.65	0.99
0.89	13.8	25.4	11.6	77.6	1.09	-1.17	0.0010	25.35	0.99

From the results in Table 1, we see that the true transition redshift is likely between 0.614 and 0.89 given the fact that the current value of the Hubble constant is known to be in that range. Thus, more

accurate measurements of the transition redshift are needed to increase the confidence of this model, though we do see that it is able to reproduce measured results.

Table 2 has the proper times from $r = u$ to the current time as well as the CMB for stationary, inertial observers ($dt = rd\Omega = 0$) by integrating Equation 20. The column τ_{tot} gives the time from $r = u$ to $r = 0$. The expression for τ_{tot} turns out to be quite simple:

$$\tau_{tot} = \frac{\pi}{2}u \quad (48)$$

Table 2. Limiting Proper Times Based on z_t Measurements and an age of 13.8 Gy for the Universe (Time is in Gy)

z_t	α_{r_0}	τ_0	τ_{tot}	τ_{remain}	τ_{CMB}
0.337	13.8	42.2	58.1	15.9	8.6
0.614	13.8	37.1	46.7	9.6	2.4
0.89	13.8	33.7	39.9	6.2	2.3

In Table 2 below, the column τ_{remain} gives the time between $r = r_0$ and $r = 0$.

Note that the proper time τ_0 of the current age of the Universe is actually much larger than the coordinate time $u - r_0$. And even though we are presently only about halfway through the “coordinate life” of the Universe (according to Table 1), the amount of proper time remaining is actually much less than the amount of proper time that has already passed (according to Table 2). This provides a measurable prediction from the model: as telescopes such as the JWST peer farther into the past with greater accuracy, we should expect to find stars, galaxies, and structures that are much older than expected because of the increased amount of proper time available for such things to form in the early Universe. Hints of this has already been found with the star HD 140283, whose age is estimated to be nearly the age of the Universe itself [5].

Next we would like to use the u and r_0 values found to create an envelope on a Hubble diagram to compare to measured supernova and quasar data. First we need to find r as a function of redshift. We can do this by solving for r in Equation 39:

$$r = \frac{u(1+z)^2}{a_0^2 + (1+z)^2} \quad (49)$$

We can derive the expression for t vs. r along a null geodesic where the geodesic ends at the current time r_0 and $t = 0$ by setting $d\tau = rd\Omega = 0$ in Equation 20 and integrating:

$$t = \int_{r_0}^r \frac{r}{u-r} dr = u \ln \left(\frac{u-r_0}{u-r} \right) + r_0 - r \quad (50)$$

Next we substitute Equation 49 into Equation 50 to get coordinate distance in terms of redshift:

$$t = r_0 + u \left[\ln \left(\frac{a_0^2 + (1+z)^2}{1+a_0^2} \right) - \frac{(1+z)^2}{a_0^2 + (1+z)^2} \right] \quad (51)$$

We need to convert the distance from Equation 51 to the distance modulus, μ , which is defined as:

$$\mu = 5 \log_{10} \left(\frac{D_L}{10} \right) \quad (52)$$

Where D_L in Equation 52 is the luminosity distance. Luminosity distance is inversely proportional to brightness B via the relationship:

$$B \propto \frac{1}{D_L^2} \quad (53)$$

The brightness is affected by two things. First, the spatial expansion will effectively increase the distance between two objects at fixed co-moving distance from each other. This will reduce the brightness by a factor of $(1+z)^2$ (because the distance in Equation 53 is squared). But there is also a brightening effect caused by the acceleration in the time dimension. We define $v \equiv \frac{d\tau}{dr} = \frac{1}{a}$ as the temporal velocity of the inertial observer at some r and the speed of light at that r as $v_c \equiv \frac{dt}{dr} = \frac{1}{a^2}$. The ratio of these velocities gives us:

$$\frac{v_c}{v} = \frac{dt}{dr} \frac{dr}{d\tau} = \frac{dt}{d\tau} = \frac{a}{a^2} = \frac{1}{a} \quad (54)$$

Equation 54 tells us how far a photon travels over a given period of time measured by the inertial observer's clock. So we see that as light travels from the emitter to the receiver, this speed decreases. This decrease in the speed from emitter to receiver will result in an increased photon density at the receiver relative to the emitter, increasing the brightness. Therefore, this effect will increase the brightness by a factor of:

$$\frac{a_0}{a} = 1 + z \quad (55)$$

This effect is not accounted for in the current relativistic cosmological models and therefore gives a second prediction that light from the distant Universe should appear brighter than expected.

Taking these brightness effects into account, the total brightness will be reduced by an overall factor of $1+z$ relative to the case of an emitter and receiver at rest relative to each other in flat spacetime. Equation 53 in terms of co-moving distance t and redshift z becomes:

$$B \propto \frac{1+z}{(t(1+z))^2} \rightarrow B \propto \frac{1}{t^2(1+z)} \quad (56)$$

Giving the luminosity distance as a function of co-moving distance t and redshift z :

$$D_L = t\sqrt{1+z} \quad (57)$$

Which gives us the final expression for the distance modulus as a function of co-moving distance and redshift:

$$\mu = 5 \log_{10} \left(\frac{t\sqrt{1+z}}{10} \right) \quad (58)$$

A plot of distance modulus vs. redshift is shown in Figure 9 below plotted over data obtained from the Supernova Cosmology Project [6]. Curves calculated from all three values of z_t in Table 1 are plotted, giving an envelope for the model's prediction of the true Hubble diagram.

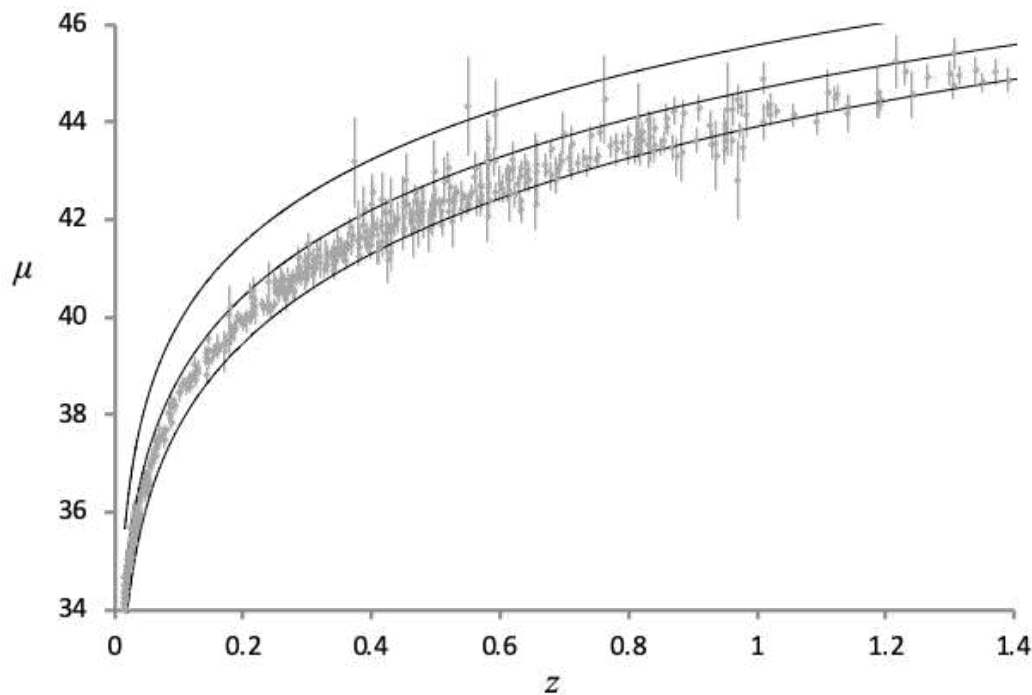


Figure 9. Distance Modulus vs. Redshift Plotted with Supernova Measurements

Note that the middle curve corresponds to $z_t = 0.614$ and the lower curve corresponds to $z_t = 0.89$. The supernova data is better fit by a curve between these values. The curve halfway between (with $z_t = 0.75$) gives us $H_0 = 71.6$, $a_0 = 1.0$, $q_0 = -1.0$, $u = 27.3$, and $r_0 = 13.5$.

In [7], the authors analyze a large sample of quasar data to obtain distance moduli at higher redshifts than is possible with supernova data. Figure 10 shows the same predicted envelope from Figure 9 for the Hubble diagram plotted out to higher redshifts with the quasar data from [7] also shown with error bars. The black diamonds in the figure are the 18 high-luminosity XMM-Newton quasar points described in [7].

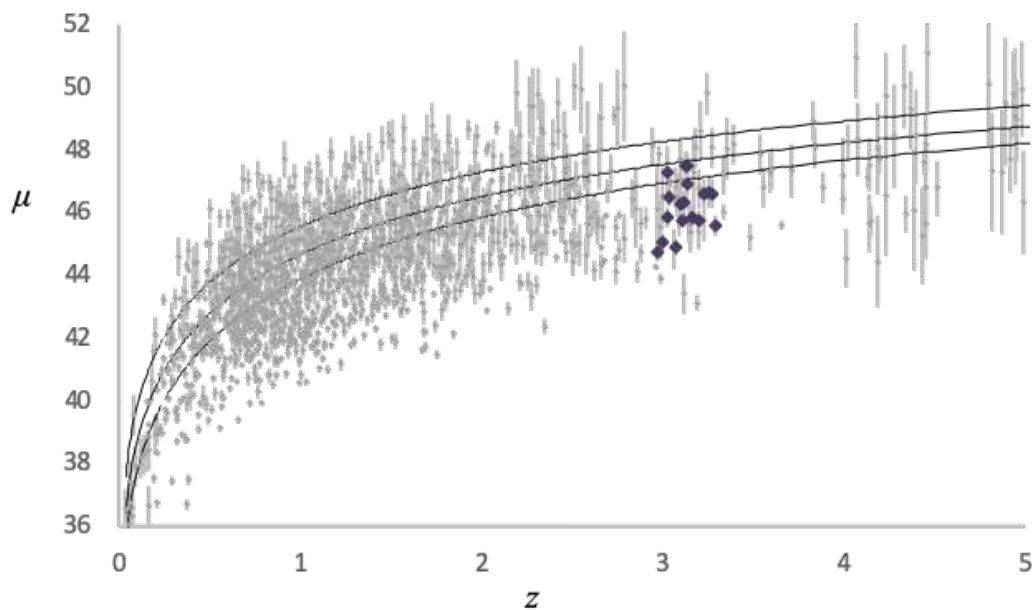


Figure 10. Distance Modulus vs. Redshift Plotted with Quasar Measurements

Finally, by subtracting r_0 from Equation 49 we can calculate the lookback time for a given redshift. Figure 11 shows the lookback time vs. redshift for the three transition redshifts.

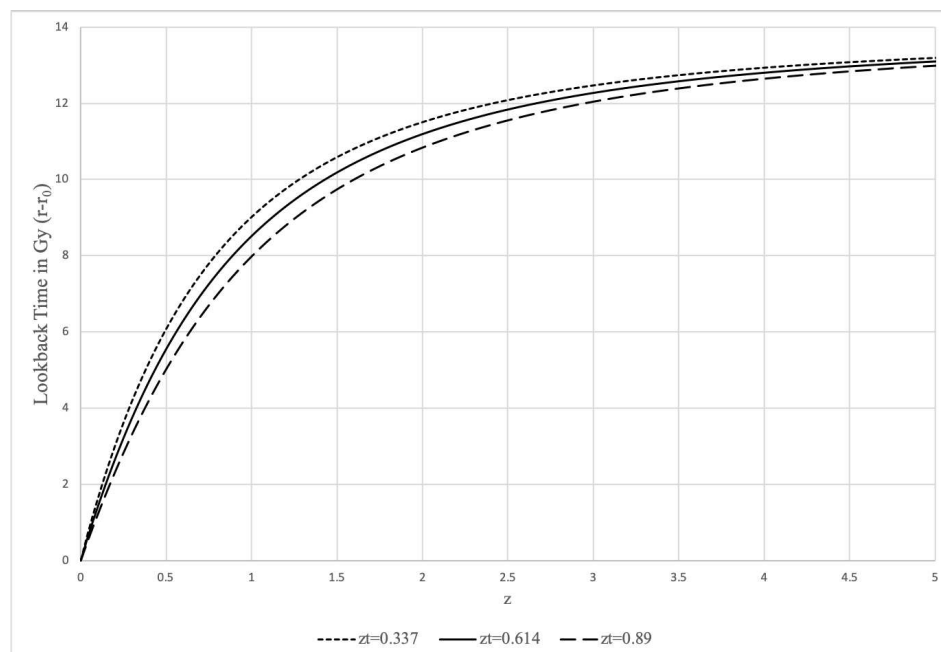


Figure 11. Lookback Time vs. Redshift

9. Understanding Cosmological Motion: A Thought Experiment

A very important fact about the internal metric is that it is not centered in space, which is consistent with the cosmological principle. The angular term of the metric, which has a center in time at all space, must be thought of differently than we usually think of spherical metrics centered in space as was discussed in Section 5. We can always put ourselves at the center of space $t = 0$ and if we pick an arbitrary direction at some fixed time r , the t dimension is a linear (not radial) dimension that extends infinitely in front of us in that direction as well as infinitely behind us in the opposite direction. So even though we are not centered in time in the metric, we can always model ourselves as being at the center of space. Understanding this is very important for visualizing what the Universe looks like when we move cosmological distances.

Imagine a Universe full of Dark Stars (for reasons that will be made apparent later, we will use the term 'Dark Stars' instead of 'Black Holes'), each one with a particle moving in the star's gravitational potential in arbitrary ways. We will focus in on one such system. Let's surround our Dark Star and particle system with a larger sphere containing both of them (call it a Cosmosphere) centered on the Dark Star and large enough that the path of the particle always remains inside it. The orientation of the system is locked to the Cosmosphere so that if the Cosmosphere moves or rotates, the system as a whole moves and rotates with it.

We already know that Equation 1 describes the path of the particle relative to the Dark Star and the r' and Ω' coordinates are measured relative to the Dark Star. But the time coordinates of Equations 1 and 20 must be related because we must be able to synchronize the times in both metrics. So we therefore need first to define the cosmological time.

The CMB shines on the Cosmosphere, and the temperature monopole of that light is directly related to the cosmological time r and therefore local time t' . When the temperature monopole is zero, we are at $r = t' = 0$. So the monopole temperature of the CMB gives us a measure of cosmological time.

We've already discussed the cosmological angular motion $\frac{d\Omega}{d\tau}$ as the Thomas Precession of the reference frame relative to the CMB. The magnitude of this spin may also be correlated to the observed

CMB quadrupole. So this leaves us with cosmological linear motion $\frac{dt}{d\tau}$. We can figure out our cosmological velocity $\frac{dt}{d\tau}$ by observing the magnitude and orientation of the temperature dipole cast on the Cosmosphere from the CMB. If the system is moving through t , one side of the sphere will be more blue than the monopole and the polar opposite side will be more red than the monopole. The Dark Star, which is at rest relative to the Cosmosphere can figure out how fast and in which cosmological direction the Cosmosphere is moving in by observing the magnitude of the dipole as well as the orientation of it.

So when an observer moves linearly in t , half the sky will be blueshifted and the other half will be redshifted and the circle perpendicular to the dipole direction will have no red or blueshift. For simplicity, let's assume all galaxies are co-moving. If we are also co-moving and we look at a set of galaxies surrounding us at a fixed $r > r_0$, these galaxies will be equally redshifted in our frame as time goes on. If we then move in t in some direction, what we would see is that we move closer to the galaxies in the blueshifted portion of the sky and away from the galaxies in the redshifted portion of the sky. How much closer or farther away we move from a particular galaxy depends on the magnitude of the red or blueshift in the direction the galaxy sits in the sky. So if we shift our position by moving in t in some direction, when we later come to rest the galaxies that originally sat on a shell equally distant in space and time from us will now each appear at different distances and times from us depending on our direction of travel. Figure 12 shows our pure motion in t on the Kruskal coordinate chart.

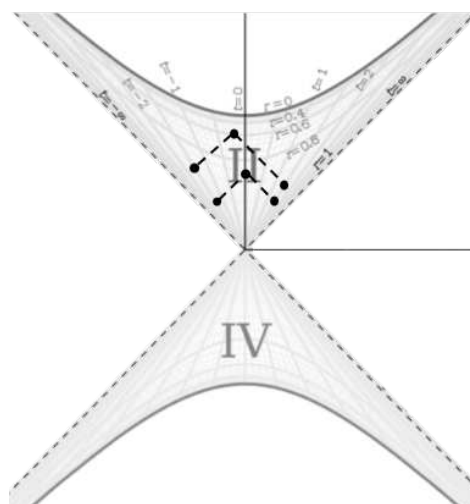


Figure 12. Depiction of Linear Cosmological Motion

Time moves upward in this diagram, so we start at $t = 0$ and see two galaxies in each direction equidistant in both space and time from us connected by equal length null geodesics (dashed lines). The galaxies we see are assumed to be co-moving in this example. Then we move in t along some direction as we fall through time. The diagram shows us how our view of the galaxies along our direction of motion changes due to this motion. When we are at some $r < r_0$ later, we no longer see the two galaxies equidistant in time and space from us. We see the galaxy we moved toward at a closer distance in both space and time to us than we did at the beginning. Conversely, we see the galaxy we moved away from at a greater distance in both space and time than we did originally (though we still see a future version of the galaxy relative to when we saw it at the beginning). But we can always define our position as $t = 0$ and we can do this by shifting the 3 points depicting the end of the motion in Figure 12 along hyperbolas of constant r by the amount t we moved. In this depiction, we would remain at $t = 0$ and the galaxies would be the things moving in our reference frame (i.e. we would hyperbolically rotate the galaxies). It would look like one galaxy is moving toward us while the other is moving away.

If we were to imagine that we are revolving around some point in space in a circle and defined our t coordinate as 0 in the Kruskal diagrams for the entire motion, the worldlines of the galaxies in all

directions would be sine waves along their lines of constant t with the phase of a given wave being a function of direction. In other words, the entire Universe would appear to wobble around us (which manifests itself as the CMB dipole sweeping across the CMB). Note that $dt \neq 0$ on a circular path since t is a hyperbolic angle, not a radius. Very importantly though, the angle we sweep as we go around that circle is not the angle in the metric. As has been discussed, the actual angle that would go into the metric would be much smaller than the angle of revolution around the point. It would be the result of the Thomas Precession caused by the angular motion. If we consider constant circular motion in the context of Figure 6, it would be described as constant motion along ∂_t while the plane rotates around ∂_ϕ at the rate of the Thomas precession of the reference frame.

In Figure 13, we show a visualization of a circular orbit to help illustrate the role of the t and Ω coordinates along a curved path (sequential parts of the cycle are numbered in ascending order).

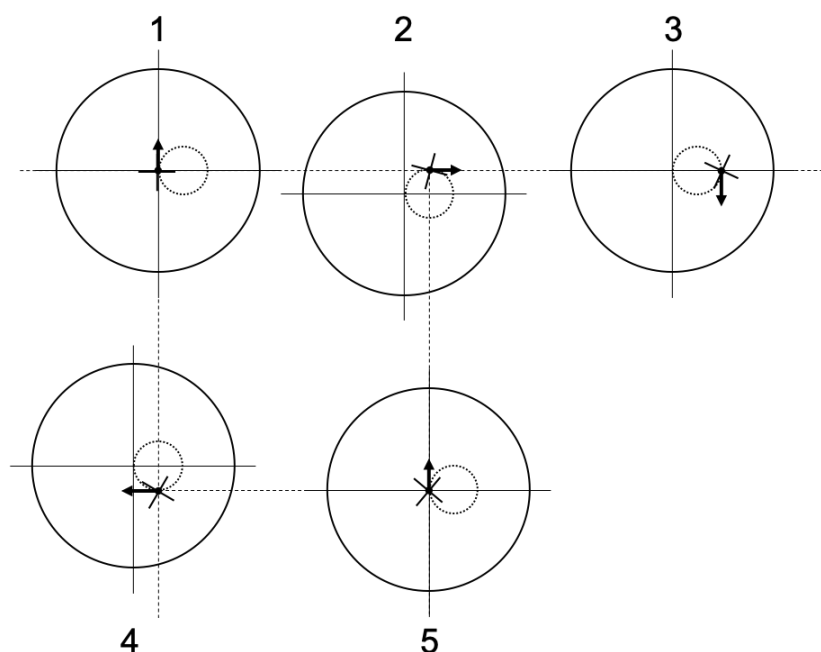


Figure 13. Visualization of Circular Orbit

At the left side of the figure, we are at the start of the orbit where the large circle represents a set of galaxies equidistant from the orbiter at that point. The smaller dashed circle represents the orbit and the arrow represents the direction of motion of the orbiter at a given moment. As we move left to right, we show the orbiter as fixed with the space moving beneath it. What is being shown here is that the best way to view the orbit is to imagine the entire space moving beneath the orbiter (the orbit and distant galaxies are fixed together and the orbit is moved beneath the orbiter). The small bold cross-hairs attached to the observer represent the orientation of the orbiter's reference frame. As we look left to right on the figure, we see these cross-hairs rotating slightly and this rotation represents the $d\Omega$ of the orbiter such that as the orbiter returns to its initial position at the far right, the cross-hairs are rotated relative to the far left of the figure.

Finally, it is important to emphasize the dt is a hyperbolic angle, not a traditional arc length or radius. So if we imagine travelling around a $t \times t$ square, we would do a hyperbolic rotation through angle t in one direction, then another hyperbolic rotation through angle t in a perpendicular direction, and so on until we return to the initial position. In the case of a circular or general curved orbit, we just do the limiting process of this where we apply continuous hyperbolic rotations through infinitesimal angles dt in continuously varying directions. This is why a circular orbit does not have a constant t (and therefore, we still see a CMB dipole while moving in a circular orbit).

10. The Anti-Universe

Figure 14 shows the full Schwarzschild metric in Kruskal-Szekeres coordinates. The diagram can be split in two along the diagonal where in the top right half, forward time points up in both the internal and external regions while in the bottom right half, forward in time points down. The direction of positive space is also swapped when looking at the upper and lower halves. For the external metric, the radius increases to the right in the upper half and to the left in the lower half. For the internal metric, the spatial t coordinate goes from $-\infty$ to $+\infty$ from left to right in the upper half and from right to left in the lower half.

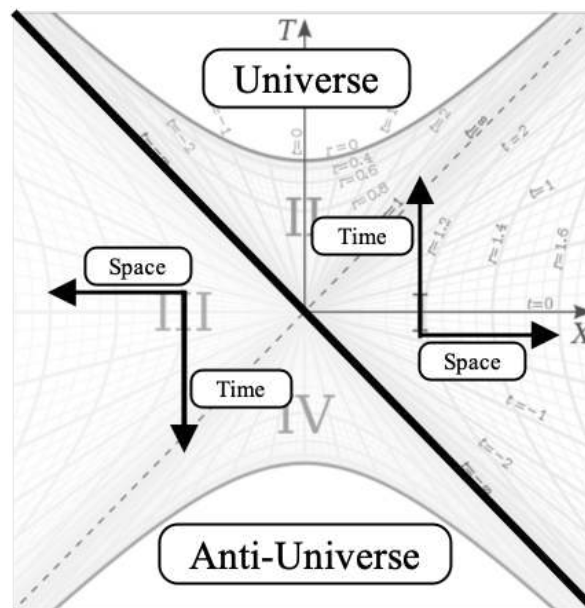


Figure 14. Universe and Anti-Universe

We can therefore conjecture that the diagram is describing both a Universe expanding up from the center and an anti-Universe expanding down from the center, each one moving toward a singularity. We expect that the anti-Universe is made of mostly anti-matter because the directions of both time and space are reversed relative to each other and therefore we expect the particles of the second Universe to have opposite charges relative to the first. This interpretation provides a resolution to the question of why we only tend to see matter in our Universe. It is because the equivalent amount of antimatter is moving away from us as a mirror Universe in the opposite direction of time. The lower hyperboloid sheet in Figure 7 therefore represents a 2D slice of the Anti-Universe at a given time.

Thus, the pair of Universes (or 'Duoverse') satisfies CPT symmetry and the Kruskal coordinates T and X in Figure 14 represent cardinal directions of space and time.

We could think of Hawking evaporation in reverse as describing the creation of the Duoverse where we start with an infinitely hot point-like horizon that ejects an infinite number of particles into the Universe and a complimentary set of anti-particles into the anti-Universe. In the next instant it expands to an infinite horizon at absolute zero in the frame of the particles that were created.

11. Newtonian Analog and the Curvature Singularity

This entire system is the temporal equivalent of two masses initially moving apart from one another until they reach a maximum separation distance u . At that point they will start falling toward each other again due to mutual gravitational attraction. When they meet at their common center, they annihilate, creating new pairs of matter/antimatter particles and begin moving away from each other again, as if they've bounced off each other. It is equivalent to the exchange of potential and kinetic Energy, but in the time dimension.

Now consider the Newtonian example of a ball in a gravitational field rising to a maximum height h and then falling back to the ground. $\frac{dh}{dt}$ will be positive on the way up, negative on the way down and zero at max height. But this also means that $\frac{dt}{dh}$ will be infinite at the maximum height because $dh = 0$ there. We might think that when comparing this to the present case, $t \rightarrow \tau$ and $h \rightarrow r$, but this is incorrect. We know that r is our time coordinate and τ is the distance along the geodesic, so $h \rightarrow \tau$ and $t \rightarrow r$. So from Equation 35, we see that, just like in the Newtonian example, $\frac{d\tau}{dr} = 0$ and $\frac{dr}{d\tau} = \infty$ at the singularity because in this case $d\tau = 0$ at the turnaround.

We can show this more explicitly for a co-moving frame. Equation 25 has constant t in this case, and we can define the velocity of the frame in T as:

$$V_T = \frac{dT}{dr} = \pm \frac{re^{\frac{r}{2u}}}{2u^{\frac{3}{2}}\sqrt{u-r}} \cosh\left(\frac{t}{2u}\right) \quad (59)$$

We take the negative solution for region II of the Kruskal-Szekeres chart since T increases when r decreases there. We can see that this velocity is $-\infty$ when $r = u$ and zero when $r = 0$. So the velocity is zero at the singularity. If we take the derivative of this velocity we get:

$$\frac{dV_T}{dr} = -\frac{e^{\frac{r}{2u}}(2u^2 - r^2)}{4u^{5/2}(u-r)^{3/2}} \cosh\left(\frac{t}{2u}\right) \quad (60)$$

Since dr is negative, this tells us that dV_T will be positive from $r = u$ to $r = 0$. But V_T is negative and therefore, the acceleration of the worldline is opposite to the velocity, causing it to decelerate in T and therefore the acceleration vector would point toward $T = X = 0$. We can also see that this acceleration is non-zero at the singularity. So if V_T is 0 at $r = 0$ and the derivative of V_T is non-zero and pointed toward $T = X = 0$ at $r = 0$, then this means that after approaching the singularity from $r > 0$ the worldline stops moving in increasing T at the singularity and begins to move in the direction of decreasing T . When the worldline then starts falling back toward $T = X = 0$, V_T is still negative, but dr is now positive. Thus dV_T will be negative, meaning the worldline accelerates toward $T = X = 0$.

Therefore, the curvature singularity represents a turnaround point for the geodesics where co-moving reference frames switch from moving in the positive direction of time to moving in the negative direction of time.

12. Condensation and Evaporation

We will now describe in detail the physical meaning behind the 'Expansion' and 'Collapse' phases of the Universe. Looking at Equation 37, we see that the $\frac{u}{r(u-r)}$ term is always positive. During the expansion phase, $\frac{dr}{d\tau}$ is negative and therefore $\frac{d^2t}{d\tau^2}$ will always be in the opposite direction of $\frac{dt}{d\tau}$. Therefore, this tells us that the peculiar velocities of cosmological objects will be reduced over time when no forces act upon them. Equation 37 describes an inertial force acting on all objects, slowing them down during the expansion phase. If the Universe is far from $r = u$ and $r = 0$, it only has noticeable effects at very large time scales and velocities (because $\frac{u}{r(u-r)} = 2H$ is very small for human velocity and time scales. For instance, currently $H \approx 71.6 \text{ km/s/Mpc}$ so converting that to $1/s$ gives a value on the order of $\sim 10^{-18}$). During collapse, $\frac{dr}{d\tau}$ is positive and now the acceleration acts in the direction of motion of the object and therefore increases its velocity over time in that phase.

So we can view the expansion phase as a condensation of the Universe. The Universe starts out as a hot plasma after the annihilation event, after which it cools and motion of the particles slow down. At the beginning of expansion, the deceleration is large (infinite at $r = u$ allowing null geodesics to become timelike), then for a long period the deceleration is small, and on approach to the singularity it once again goes to infinity. For just a moment at the singularity, all motion stops completely. The particles stop completely at the singularity because $\frac{u}{r(u-r)}$, $\frac{dr}{d\tau}$ and therefore $\frac{d^2t}{d\tau^2}$ become infinite there putting an infinite inertial drag force on all objects. This is true even for objects with a

proper acceleration. So the expansion counter-intuitively effectively stabilizes gravitational structures more and more as time moves forward, promoting this condensation.

Likewise, the collapse phase can be viewed as an evaporation. After condensation, the Universe begins the collapse phase. As the Universe emerges from the singularity, the inertial force that now tends to accelerate is extremely large (falling from infinity at the singularity), but the $\frac{dt}{d\tau}$ of everything is zero, so there is no initial acceleration at the very beginning of collapse. But any perturbation to a particle's state of rest will induce an inertial acceleration in the direction of motion. Therefore, particles will naturally gain momentum over time and the Universe will heat up as gravitationally bound structures begin to break down and the Universe tends back toward a state of hot plasma as it approaches the annihilation event. Once again $\frac{u}{r(u-r)}$, $\frac{dr}{d\tau}$ and therefore $\frac{d^2t}{d\tau^2}$ become infinite at the annihilation event, sending all particles toward light-like geodesics as though they effectively lose all their mass.

Now let us consider this from the perspective of the external metric. Consider a star that has collapsed to form a Black Hole. As will be demonstrated, the star can never actually form an event horizon, but we can imagine that the star is massive enough that it becomes a 'Dark Star'.

The Schwarzschild metric depicted in Figure 1 describes an 'eternal' Dark Star. But we could also say that it describes a Dark Star from the beginning of the Universe to the end of the Universe, with the beginning of the Universe being marked by the $t' = -\infty$ line and the end being the $t' = \infty$ line. The Schwarzschild metric is asymptotically Minkowskian, so it does not truly represent the spacetime around a real spherically symmetric mass since the background Universe has been observed to be non-Minkowskian, but we can use this metric along with what has been determined from Equation 37 to approximate the expected trajectory for a freefalling object in the field of a Dark Star over the expansion and collapse phases of the Universe. The path $\frac{dr'}{dt'}$ of an object in freefall in the field of a Dark Star as seen by a distant observer is given by [8]:

$$\frac{dr'}{dt'} = \pm \left(\frac{r' - r_s}{r'} \right) \sqrt{\frac{r'_0(r'_0 - r')}{r'(r'_0 - r_s)}} \quad (61)$$

Where r'_0 is the radius at which the object begins falling from rest and r_s is the Schwarzschild radius. The focus here is not on the equation itself, which is a well-known solution, but at the \pm in front of it that comes from taking the square root. We first note that dt' in the external metric is the proper time interval of an observer at infinity. In the cosmological case, this interval is the proper time of the co-moving observer $dt' = d\tau_{co-moving} = \pm \frac{1}{a} dr$. Therefore, we can modify Equation 61 as follows:

$$dr' = \pm \frac{1}{a} dr \left(\frac{r' - r_s}{r'} \right) \sqrt{\frac{r'_0(r'_0 - r')}{r'(r'_0 - r_s)}} \quad (62)$$

For an observer falling in the external metric from some $t' < 0$, dt' is always positive. But we know that dr is negative during expansion and positive during collapse. Therefore, if we take the positive root of Equation 62, we see that during expansion dr' will be negative (because dr is negative) and during collapse dr' will be positive. We assert that the time at which the Universe changes from expansion to collapse is at $t' = 0$ and therefore the expansion occurs in the $t' < 0$ region and collapse occurs in the $t' > 0$ region.

So during collapse, freefalling objects are ejected symmetrically out of the gravitational field of the object relative to expansion. We also note that at $t' = r = 0$, $a \rightarrow \infty$ and therefore $dr' = 0$. So we can say that as an object approaches $t' = 0$, its worldline must become tangent to the r' hyperbola closest to it. And as collapse begins, it will smoothly and symmetrically curve in the opposite direction. Furthermore it should be noted that since the expansion phase takes place in the $t' < 0$ region, an event horizon can never form because that would require faster than light motion to achieve.

An approximate example of a real geodesic for an object in freefall in such a gravitational field is shown by the dark black line in Figure 15 through both the expansion and collapse phases of the Universe.

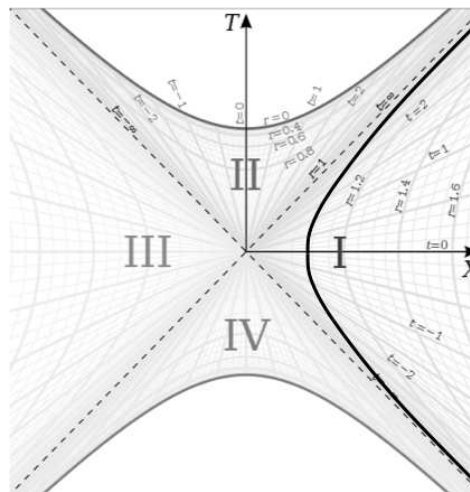


Figure 15. Schwarzschild Freefall in Expanding and Collapsing Spacetime

The conclusion we can draw from this is as follows. During expansion, the background of the Universe glows with decreasing temperature and brightness over time via the CMB as gravitational structures stabilize and galaxies form. During this phase, some stars will collapse to form Dark Stars that we presently think of as Black Holes. By the time we reach the singularity, the Universe will be fully condensed and inert. At the singularity, light from the CMB will be infinitely redshifted such that it is no longer detectable and the background Universe becomes black (because a_0 in Equation 39 becomes infinite there). The observer will see a completely dark Universe at the singularity and over time, the Dark Stars will begin to glow like candles lighting up the darkness as the geodesics of the particles that were falling toward their centers during expansion reverse and now move outward (unabsorbed light will also be reflected back outward during collapse). Shadow becomes flame. These former "Black Holes" effectively become "White Holes", with matter radiating from them, seemingly out of the vacuum, even though the radiation is coming from matter that had accumulated in that region during expansion. As the collapse proceeds, these White Holes will grow brighter and shrink as the matter and energy making them up escapes to the external Universe at higher and higher energies due to the increasing inertial acceleration from Equation 37. The Universe effectively evaporates as all gravitational structures break down. By the end of collapse, the Universe has returned to a state of increasingly dense plasma until it collides with the anti-Universe at the annihilation horizon.

We can summarize as follows: We know from Equation 37 that the worldlines of all matter become null at the end of collapse, so by symmetry, they will begin the expansion as null geodesics as well at $r = u$. They enter the singularity parallel to the t coordinate per Equation 37 at the end of expansion. The geodesics then begin to move from $r = 0$ to increasing r during the collapse (interpretation of the infinite curvature is given in Section 11), accelerating inertially over time per Equation 37. Observers are inertially accelerated to become null geodesics as they approach the annihilation event at the end of collapse per Equation 37.

Note that if the Universe collapses over the same manifold on which it expanded, this would suggest we live in a 'presentist' Universe as opposed to a 'block' Universe because if that were not true, the collapsing matter would collide with the expanding matter.

13. Total Proper Time

The proper time in Equation 1 implicitly assumes the local gravitational field is in a co-moving cosmological frame. This is because t' must be a function of cosmological time r . In fact, we know that

as $r' \rightarrow \infty$ the proper time interval of the co-moving observer $d\tau$ has to be equal to the t' interval, we can choose dt' to be $dt' = d\tau_{\text{co-moving}}$. But there is no reference to the spacelike t and Ω cosmological dimensions in the internal metric. If the source of the gravitational field has cosmological motion, the true proper time will be reduced relative to Equation 1 due to time dilation effects. The total proper time interval is found by multiplying $d\tau'$ by the ratio of $\frac{d\tau}{dr}$ for the actual cosmological motion of the field source and $\frac{d\tau}{dr}$ of a co-moving frame:

$$d\tau_{\text{tot}} = d\tau' \frac{d\tau}{dr} \left(\frac{dr}{d\tau} \right)_{\text{co-moving}} \quad (63)$$

Which becomes:

$$d\tau_{\text{tot}} = d\tau' \sqrt{1 - \left(a^2 \frac{dt}{dr} \right)^2 - \left(ar \frac{d\Omega}{dr} \right)^2} \quad (64)$$

Recognizing that $\frac{1}{a^2}$ is the linear cosmological speed of light (Equation 36), we can define $\frac{dt}{dr} \equiv v$ and the cosmological linear speed of light $\frac{1}{a^2} \equiv v_c$. We also define the angular speed $\frac{d\Omega}{dr} \equiv \omega$ and the cosmological angular null geodesic as $\frac{1}{ar} = \omega_c$ (by solving for $\frac{d\Omega}{dr}$ in Equation 20 with $d\tau = dt = 0$), then we can write Equation 64 as:

$$d\tau_{\text{tot}} = d\tau' \sqrt{1 - \left(\frac{v}{v_c} \right)^2 - \left(\frac{\omega}{\omega_c} \right)^2} \quad (65)$$

If we multiply $\frac{\omega}{\omega_c}$ by $\frac{r}{r}$, and recognize that $\left(\frac{v}{v_c} \right)^2 + \left(\frac{r\omega}{r\omega_c} \right)^2 \equiv V^2$ is the total cosmological velocity (because $r\omega$ is the tangential velocity which is perpendicular to the linear velocity), then we recover the Minkowski form of the length contraction equation where the speed of light varies over cosmological time:

$$d\tau_{\text{tot}} = d\tau' \sqrt{1 - V^2} \quad (66)$$

This is telling us that the worldlines in metrics such as the external Schwarzschild metric are contracted by the system's cosmological motion. So we see that the cosmological model is essentially a collection of systems described by metrics like the external Schwarzschild metric in a hyperbolic background that is a quasi-Minkowski metric with a time dependant speed of light.

In order for Equation 65 to be real, the quantity under the square root must be positive and therefore

$$v \leq v_c \sqrt{1 - \left(\frac{\omega}{\omega_c} \right)^2} \quad (67)$$

And so we see that the upper speed limit of an object depends on its spin. In other words if an object is spinning about the time dimension while moving in a straight line, its maximum speed will be reduced per Equation 67. It's as though this spin has increased the mass of the particle, and perhaps even gives mass to a massless particle. The mass would be related to the precession of the inertial frame about the time axis.

14. 'Spaghettification', and a Self Portrait of the Universe

We will now take a closer look at what actually happens at the singularity in the cosmological context. When approaching the singularity, the $d\Omega$ term vanishes and proper distances go to infinity. This is often referred to as 'spaghettification'. In the conventional context of falling into a Black Hole, this is interpreted as an observer approaching the singularity getting both infinitely stretched and squeezed and then they just cease to exist at the singularity. But when we interpret the internal metric as the cosmological solution, we find that the true nature of the metric behavior at the singularity is in fact much more mundane, yet incredibly revealing.

Let us now consider the singularity. The light cone opening angle ψ at a given cosmological time is given by:

$$\psi = 2 \tan^{-1} \left(\frac{dt}{dr_{\text{light}}} \right) = 2 \tan^{-1} \left(\frac{1}{a^2} \right) \quad (68)$$

Figure 16 shows the light cone angle ψ as function of r as we move along the r axis with decreasing r during expansion, through the singularity, and then in increasing r during collapse.

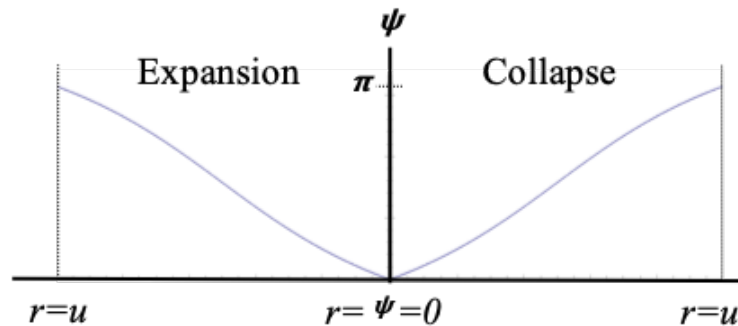


Figure 16. Local light cone angles over time

We begin expansion at the left side of the diagram where the light cone is totally open ($\psi = \pi$), because Equation 36 goes to ∞ there. As we move through time, the angle closes until at the singularity, light no longer travels through t ($\psi = 0$), which is why Equation 36 goes to zero there. At the singularity, light no longer travels through space and everything becomes spacelike. But also recall that motion has stopped at this point and all light is infinitely redshifted, so there isn't really a physical stretch happening, it's only that adjacent points in space are unable to communicate with each other at that instant. Then as we pass the singularity and continue moving now with increasing r during collapse, the light cone will start opening in a symmetric way to how it closed during expansion.

Therefore, space is not expanding the way we currently think about it in terms of a stretching of space. What is changing is how quickly different points in space are able to communicate with each other. The image of space itself compressing to a point or ripping itself apart is misleading. At the beginning of expansion, we have a normal 3D space of particles that can communicate instantly with all other particles regardless of distance because the speed of light is infinite there. This communication speed drops as expansion proceeds and local gravitational structures are able to form. When reaching the singularity where the scale factor is infinite, space is not ripped apart but rather the light cone angles have closed completely such that adjacent regions of space are unable to communicate with each other which manifests as infinite proper distances.

Data Availability Statement: All data generated or analysed during this study are included in this published article [and its supplementary information files].

Statements and Declarations: There are no competing interests.

References

1. Carroll, S.M. Lecture Notes on General Relativity, 1997, [arXiv:gr-qc/9712019v1].
2. Figures 1, 2, and 3 are modifications of: 'Kruskal diagram of Schwarzschild chart' by Dr Greg. Licensed under CC BY-SA 3.0 via Wikimedia Commons. http://commons.wikimedia.org/wiki/File:Kruskal_diagram_of_Schwarzschild_chart.svg#/media/File:Kruskal_diagram_of_Schwarzschild_chart.svg, Accessed in 2017.
3. Raine, D.; Thomas, E. *Black Holes a Student Text*; Imperial College Press, 2015.
4. Lima, J.A.S.; Jesus, J.F.; Santos, R.C.; Gill, M.S.S. Is the transition redshift a new cosmological number?, 2014, [arXiv:astro-ph.CO/1205.4688].

5. Bond, H.E.; Nelan, E.P.; VandenBerg, D.A.; Schaefer, G.H.; Harmer, D. HD 140283: A STAR IN THE SOLAR NEIGHBORHOOD THAT FORMED SHORTLY AFTER THE BIG BANG. *The Astrophysical Journal* **2013**, 765, L12. doi:10.1088/2041-8205/765/1/L12.
6. Supernova Cosmology Project - Union2.1 Compilation Magnitude vs. Redshift Table (for your own cosmology fitter). <http://supernova.lbl.gov/Union/figures/SCPUnion2.1muvsz.txt>, 2010. Accessed on Aug. 17, 2017.
7. Risaliti, G.; Lusso, E. Cosmological constraints from the Hubble diagram of quasars at high redshifts, 2018, [arXiv:astro-ph.CO/1811.02590].
8. Augousti, A.; Gawelczyk, M.; Siwek, A.; Radosz, A. Touching ghosts: Observing free fall from an infalling frame of reference into a Schwarzschild black hole. *European Journal of Physics - EUR J PHYS* **2012**, 33, 1–11. doi:10.1088/0143-0807/33/1/001.

Disclaimer/Publisher's Note: The statements, opinions and data contained in all publications are solely those of the individual author(s) and contributor(s) and not of MDPI and/or the editor(s). MDPI and/or the editor(s) disclaim responsibility for any injury to people or property resulting from any ideas, methods, instructions or products referred to in the content.